Vortex molecules in spinor condensates

Ari M. Turner[1,2] and Eugene Demler[1]
[1]*Department of Physics, Harvard University, Cambridge, Massachusetts 02138, USA*
[2]*Department of Physics, University of California, Berkeley, California 94720, USA*
(Received 7 August 2008; revised manuscript received 20 April 2009; published 22 June 2009)

Condensates of atoms with spins can have vortices of several types; these are related to the symmetry group of the atoms' ground state. We discuss how, when a condensate is placed in a small magnetic field that breaks the spin symmetry, these vortices may form bound states. Using symmetry classification of vortex charge and rough estimates for vortex interactions, one can show that some configurations that are stable at zero temperature can decay at finite temperatures by crossing over energy barriers. Our focus is cyclic spin-2 condensates which have tetrahedral symmetry.

DOI: 10.1103/PhysRevB.79.214522 PACS number(s): 03.75.Mn, 75.70.Kw, 61.30.Jf, 11.27.+d

I. VORTEX MOLECULES AND ASYMMETRY

In an image of a nematic liquid crystal by polarized light, one can identify defects in the nematic order with various topological charges.[1,2] Bose condensates (see the books[3,4]) form another "material" which can have topological defects. In a spinor condensate,[5–7] both the phase *and* spin textures may be disrupted by defects.[8] (See also Refs. 9 and 10 for reviews of spinor condensates.)

A topological defect in the *phase* of a superfluid is a quantized vortex. If the circulation of a vortex is $n\frac{h}{m}$, then the discontinuity in the phase as the defect is encircled is $2\pi n$. In a single-component superfluid, multiply-quantized vortices ($|n|>1$) are usually not stable. The widely known explanation is that the energy of a vortex is proportional to n^2. Thus a doubly-quantized vortex ($n^2=4$) can lower its energy by splitting into two singly-quantized vortices. Similar arguments can be formulated for multicomponent condensates, but we will find that some vortices in these condensates can be very long lived in spite of having large energies. These metastable vortices should occur in condensates of atoms with spin with imperfect rotational symmetry. A small parameter q, such as the interaction between the spins and the magnetic field, describes the *weak* disruption. (We focus on the *cyclic* condensates of spin-2 atoms, see Ref. 11.)

Long-lived multiply-quantized vortices are particular examples of composite vortices, vortices that are made up of several vortices bound together. Ground states with complicated symmetries have many types of vortices, which can be classified using group theory.[12] Symmetry-violating fields provide a force that can bind such vortices together so that they form a "composite core" for a larger vortex, as shown previously for vortices in He^3.[13,14] For a small value of q, the composite core will consist of a set of vortices held loosely together.

As q increases, this structure will contract so that it looks more like a vortex with a single asymmetrical core. Asymmetrical vortices and composite vortices occur in many contexts. The vortex-bound states in He^3 have actually been found.[15,16] For He^3, the asymmetry is produced by the dipole-dipole interaction (which correlates spin and orbital angular momentum) and the interaction with the magnetic field. Turning to condensates, Ref. 17 predicts vortices for a Bose-condensed gas of two atomic states when there is an rf field producing coherent transitions between the states. The binding of these vortices also comes from an asymmetry, but the asymmetry comes from the dependence of the interaction strength on the internal states of the atoms rather than from an external magnetic field. Reference 18 studied vortices of spinor atoms in a magnetic field and described composite vortices as we do. Since the scenario involves rotation as well as a magnetic field, the vortices would be held close to the *axis* of the condensate by rotational confinement without the magnetic field. With just a magnetic field, we show that the vortices are still attracted to *one another*.

The vortices and the bound states they form are not hard to picture by taking advantage of the fact that the state of a spinor atom can be represented by a geometrical figure. The appropriate shape depends on the type of condensate. For a ferromagnetic condensate, a stake pointing in the direction of the magnetization can represent the local state of the condensate. Other condensates can be represented by more complicated shapes. Now imagine a plane filled with identical shapes (tetrahedra, for the cyclic phase), with orientations varying continuously as a function of position, as in Fig. 6. This shape field (or "spin texture") together with a phase field represents a nonuniform state of a condensate. If the shapes rotate around a fixed symmetry axis as some point is encircled then the spin texture has a topological defect at this point (see Ref. 12 for the theory of defects). Such configurations generalize vortices because they are accompanied by persistent spin or charge currents. For each symmetry of the tetrahedron, there will be a vortex when the Hamiltonian is SU_2 symmetric; we call such vortices "tetrahedral" vortices because their order parameters explore the full space $\mathcal{M}$ of orientations of a tetrahedron. The types of vortices in the cyclic phase have been classified in Refs. 19 and 20. (Each discrete subgroup of SU_2 describes the vortices of some phase for atoms of some spin;[21] to find vortices for more even more complicated groups such as SO_5 or SO_7, one might want to study gases of spin-$\frac{3}{2}$ atoms.[22,23])

Any tetrahedral vortex can exist when there is no magnetic field, but when a magnetic field is applied, the vortex spectrum is decimated. The tetrahedra can rotate only around the magnetic field direction. To understand this, note, for example, that in the cyclic phase, the tetrahedra prefer to

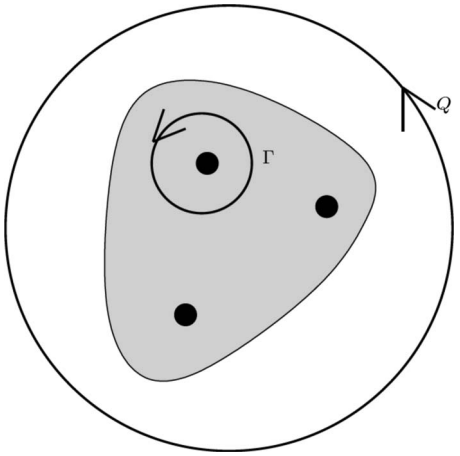

FIG. 1. A composite vortex reflects the hierarchy of the order-parameter space. The size of a region increases as the energy scale of its order parameter decreases. In the white, gray, and black regions the order parameter moves from $\mathcal{M}_q$ to $\mathcal{M}$ to $\mathcal{H}$. The charges of the subvortices are tetrahedral charges, represented by Γ, and the charge of the composite vortex is a field-aligned charge.

have an order-3 axis along the magnetic field (for appropriate atomic parameters). Therefore the magnetic field *rejects* vortices based on the other symmetry axes. The "field-aligned" vortices, where the distant tetrahedra stay in the $B \neq 0$ ground-state space $\mathcal{M}_q$, are the only ones which the field allows.

Even when a nonzero field rejects them, tetrahedral vortices can form stable composite vortices. Because of the way vortex charges "add" when several objectionable vortices are placed together, their combined field *can* align with the magnetic field beyond a great enough distance. Such a family of vortices will form a stable configuration within the condensate. The alignment condition keeps the vortices from separating, and, in some cases, the "Coulomb" repulsion between them keeps them from merging. Considered as a whole, these vortices form the core of a composite *field-aligned* vortex (Fig. 1).

A composite vortex is like the pulp and seeds of a fruit. As emphasized in research on helium-3 vortices,[13] the structure of such a fruit reflects the hierarchy of the order-parameter space, with its nested subspaces, of increasing energy scales: $\mathcal{M}_q$, $\mathcal{M}$, and $\mathcal{H}$ (the whole Hilbert space, corresponding to arbitrarily *distorted* tetrahedra). The seeds are where the order parameter is in $\mathcal{H}-\mathcal{M}$ (i.e., the tetrahedra are distorted) and the pulp is where the order parameter is in $\mathcal{M}-\mathcal{M}_q$ (i.e., the tetrahedra have arbitrary orientations). Thus, the texture in the pulp (or composite core) behaves qualitatively as if $q=0$ and the seeds are the cores of tetrahedral vortices.

Some of the vortex molecules for the cyclic phase are metastable. Reference 18 mentions an interesting clue to such a phenomenon; namely, there are multiple steady-state wave functions describing a condensate with a given magnetization and rotational frequency. These local minima of the energy function can maybe be analyzed using the group-theoretic binding conditions we discuss in Sec. V D. For a spinor condensate, wave functions for states besides the ground state are experimentally important since the experiments of Ref. 8, as well as the liquid crystal experiments of Ref. 2, reveal complicated textures produced by chance; an initial fluctuation around a uniform excited state becomes unstable and evolves into an intricate *nonequilibrium* texture. So it is useful to analyze spin textures which (like the metastable vortex molecules considered here) are only *local* minima of the Gross-Pitaevskii energy functional as well as unstable equilibria considered in Ref. 24 (which take a long time to fluctuate out of their initial configuration). The process by which textures form out of uniform initial states has been discussed in theoretical articles, including Refs. 25 and 26, on the statistics of the spin fluctuations and vortices that are produced from this random evolution, Ref. 27, on the spectrum of instabilities, and Refs. 28 and 29 on the dynamics of spinor condensates. The experiments described in Ref. 30 show that the patterns that evolve in rubidium condensates are probably affected by dipole-dipole interactions, though we are not considering these. Dipole-dipole interactions lead to antiferromagnetic phases,[31] which maybe can be described as *ground-state* configurations of vortices.

Besides just hoping for unusual types of vortices to form, one can make a vortex lattice by rotating a condensate. The vortices in a rotating multicomponent condensate have been investigated theoretically in Ref. 32 for a two-component or spin-1 condensate and Ref. 33 for a cyclic condensate. Experiments can also make a single vortex of a prescribed type.[34–36] Excited by these possibilities, physicists have come up with several types of vortices and topological defects they would be interested in seeing: skyrmions,[37,38] monopoles,[39] and textures whose order-parameter-field lines make linked loops,[40] as well as the noncommutative vortices of the cyclic phase whose bound states we will be studying here.

II. OVERVIEW

The behavior of vortex molecules can be understood by focusing on one example, as we do in this section. The remainder of the paper provides a more complete discussion and gives more detailed predictions. The two sections after this one present the basic properties of the cyclic phase: Sec. III summarizes the noncommutative group theory of combining vortex charges and the classification of the tetrahedral vortices; Sec. IV estimates the elastic energies and Zeeman energies of such clusters as functions of the charges of the vortices. Next, Sec. V describes the chemistry of molecules, giving formal criteria which determine what types of tetrahedral vortices form bound states or metastable states. The last two sections illustrate the general approach with some surprising examples (Sec. VI) and give some basic ideas about how to observe metastable vortices (Sec. VII). The reader can focus on the *concepts* introduced in this section as well as the formal statement of the binding criteria (Sec. V C), together with some of the *applications*—the decay paths of metastable molecules (see Sec. V D), additional types of vortex molecules (Sec. VI), or possible experiments.

A. Picturing the cyclic state

The key to our discussion of vortices in a cyclic condensate is the geometrical representation of a cyclic state

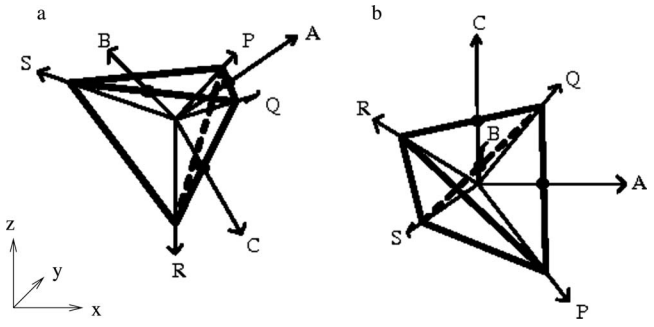

FIG. 2. Geometrical representation of the cyclic phase. Two orientations of a tetrahedron, corresponding to the spin nodes of the ground-state spinor, are illustrated and the symmetry axes are labeled. The magnetic field is along the z axis (see the coordinate axes at left). (a) An orientation with the magnetic field along an order-3 axis, corresponding to the ground state $\sqrt{n_0}\chi_3$ for $c>4$. (b) An orientation with the magnetic field along an order-2 axis, corresponding to the ground state for $c<4$, $\sqrt{n_0}\chi_2$ [see Eq. (34)]. Note that the three order-2 axes A, B, and C are orthogonal so they can be used as a set of body axes.

by a tetrahedron (see Fig. 2). Without this representation, a spin texture would be given by a spinor field $[\psi_2(x,y),\psi_1(x,y),\psi_0(x,y),\psi_{-1}(x,y),\psi_{-2}(x,y)]^T$; the fact that this spinor lies in the ground-state manifold $\mathcal{M}$ would have to be described by a set of polynomial relations between the five components. A more revealing way to represent a spinor is to draw a geometrical figure consisting of "spin nodes" (as in Ref. 41) and in the cyclic phase, these spin nodes form the vertices of a tetrahedron. (A similar construction can be used to classify vortices in condensates of spin-3 atoms, see Ref. 42.) Even without using the spin-node interpretation, one can justify using tetrahedra to represent order parameters in the cyclic phase because they are a concrete way of representing the symmetry of this phase. Reference 19 found the symmetry group of a state in the cyclic phase by finding all the pairs $\hat{\boldsymbol{n}},\alpha$ such that

$$e^{-i\alpha \boldsymbol{F}\cdot\hat{\boldsymbol{n}}}\chi_3 \propto \chi_3, \tag{1}$$

where $\boldsymbol{F}$ is the vector of spin-2 matrices (representing the hyperfine spin of the atoms) and

$$\chi_3 = \begin{pmatrix} \sqrt{\frac{1}{3}} \\ 0 \\ 0 \\ \sqrt{\frac{2}{3}} \\ 0 \end{pmatrix}. \tag{2}$$

The spinor $\sqrt{n_0}\chi_3$ is a representative cyclic state if n_0 is the density of the condensate. The symmetry axes for this spinor turned out to be the same as those for the tetrahedron in Fig. 2(a). The other ground states are obtained by applying rotation matrices in spinor space. They are represented by the corresponding rotation of the tetrahedron.

B. Distortions due to the magnetic field

The Hamiltonian for spin-2 atoms in a magnetic field is

$$\mathcal{H} = \int\int d^2\mathbf{u}\left[\frac{\hbar^2}{2m}\nabla\psi^\dagger\nabla\psi + V_{tot}(\psi)\right]. \tag{3}$$

The potential V_{tot} has a simple expression[11] in terms of the density $n=\psi^\dagger\psi$, magnetization $\mathbf{m}=\psi^\dagger\mathbf{F}\psi$, and singlet-pair amplitude $\theta=\psi_t^\dagger\psi$ (ψ_t stands for the time reversal of ψ),

$$V_{tot}(\psi) = \frac{1}{2}(\alpha n^2 + \beta\mathbf{m}^2 + c\beta|\theta|^2) - q\psi^\dagger F_z^2\psi - \mu\psi^\dagger\psi, \tag{4}$$

where α, β, c, q, and μ are parameters; μ is the chemical potential. The first three terms describe the rotationally symmetric interactions of pairs of atoms. The first one describes repulsion between a pair of atoms and the next two terms describe additional, smaller interactions that depend on the spin states of the two colliding atoms. These terms determine the ground state in the absence of a magnetic field, worked out by Ref. 11. The cyclic phase occurs when β and c are positive. (The spin-dependent interaction strengths $\beta, c\beta$ can be expressed in terms of differences of the scattering lengths.) Spin-2 and spin-1 atoms in a rotationally invariant trap have been investigated experimentally in Refs. 8 and 43–46; Ref. 47 reviews more experimental phenomena. References 44 and 45 found values for α, β, and c for ^{87}Rb that are consistent with theoretical predictions, although even the sign of c is not known for sure because c is small. Rubidium is the closest element so far condensed to having a cyclic ground state, but c is still believed to be negative, unless some type of field is applied to adjust its value. Our theory applies to atoms in the cyclic phase and we assume furthermore that c is of order 1 and that $\beta \ll \alpha$ to justify some approximations.

The ground-state orientations in a magnetic field are chosen from $\mathcal{M}$ by the quadratic Zeeman shift, which is the fourth term of the energy function. For a magnetic field B along the z axis, $q \propto B^2$. (See Ref. 3 for the explanation of why the quadratic Zeeman term q but not the linear term is relevant if the condensate's initial magnetization is zero. A nonzero magnetization is described by a Lagrange multiplier term $-p\int\int d^2\mathbf{x}\psi^\dagger F_z\psi$, which looks like a linear Zeeman coupling. We assume $p=0$; a small p should also produce some vortex-bound states, since, like q, it breaks the rotational symmetry.)

When $B\neq 0$, the Zeeman effect gives rise to an extra subdivision of the cyclic phase into two phases according to whether $c>4$ or $c<4$. (Different transitions occur at very low magnetic fields.[33]) The two phases can be found (see Sec. IV A) by finding how the energy of a cyclic state varies as a function of the orientation of the corresponding tetrahedron

$$V_{eff} = (c-4)\frac{3q^2}{4c\beta}(\cos^4\alpha_1 + \cos^4\alpha_2 + \cos^4\alpha_3), \tag{5}$$

where α_1, α_2, and α_3 are the angles between the z axis and three-body axes A, B, and C fixed to the tetrahedron [see Fig. 2(a)]. When $q\neq 0$, there is a phase transition at $c=4$, though there is nothing special about $c=4$ in *zero* magnetic field. The ground-state orientation of the tetrahedron has order-3 symmetry when $c>4$ and order-2 symmetry when $c<4$, as

TABLE I. Examples of vortex molecules. The tetrahedral charges of the components of the molecules and the net-aligned charge are given using the notation from Sec. III B. The condition on c describes which phase the condensate has to be in for each molecule to be realized. The second molecule might actually not be bound (see Sec. VI A).

	Components	Net Charge	c	Stable?
1	$(A,0)*(A,0)$	$(2\pi,0)_3$	$c>4$	Metastable
2	$(P^{-1},\frac{4\pi}{3})*(Q^{-1},\frac{4\pi}{3})*(R^{-1},\frac{4\pi}{3})$	$(0,4\pi)_2$	$c<4$	Metastable
3	$(Q,\frac{2\pi}{3})*(A,0)$	$(-\frac{4\pi}{3},\frac{2\pi}{3})_3$	$c>4$	Stable
4	None	$(4\pi,0)_{2,3}$	Any value	Metastable

illustrated in Figs. 2(a) and 2(b). When $c>4$ the absolute ground-state space $\mathcal{M}_q=\mathcal{M}_{q3}$ contains all rotations about the z axis (combined with rephasings) of $\sqrt{n_0}\chi_3$, which have energy $V_{effective}=V_{\min}=\frac{(c-4)q^2}{4c\beta}$.

C. Vortex molecule

This paper will predict several vortex molecules which are stabilized by magnetic fields—some for each of the phases illustrated in Fig. 2; these molecules are listed in Table I. We will mostly assume $c>4$ until we have discussed the first molecule in the table thoroughly.

Consider a single vortex associated with the rotation through 180° of the ground-state tetrahedron [see Fig. 2(a)] about the A axis, which is not parallel to the magnetic field, $(\sqrt{\frac{2}{3}},0,\sqrt{\frac{1}{3}})$. This vortex is described at large distances by

$$\psi(r,\phi)=e^{-i(\phi/2)(1/\sqrt{3})(\sqrt{2}F_x+F_z)}\sqrt{n_0}\chi_3, \tag{6}$$

where r,ϕ are polar coordinates centered on the core of the vortex. Such a vortex will be expelled by the condensate if $c>4$ because its excess Zeeman energy density (relative to the ground-state energy of the condensate $V_{\min}$) diverges with the condensate size. According to Eq. (5) the energy is[48]

$$\frac{(c-4)(q^2)}{6\beta c}(\sin^2\phi). \tag{7}$$

The tetrahedra are pointing in a direction disfavored by the magnetic field (except the ones lined up along the positive and negative x axis). The integrated energy is proportional to the area

$$E_{\text{misalign}}\sim\frac{q^2R^2}{\beta c}, \tag{8}$$

where R is the condensate's radius.

A vortex based on a 180° symmetry cannot be the only vortex in an infinite condensate, but it can form a partnership with another vortex of the same type, producing a molecule that can exist without costing too much energy. This is because the *net charge* of two of these vortices is compatible with the magnetic field. The combination of two 180° rotations of the tetrahedral order parameter about the A axis is a 360° rotation about the A axis, but since any rotation axis is a 360° symmetry of the tetrahedron, this rotation axis can change continuously on larger and larger circles. It can tilt *relative to the tetrahedra* so that at large distances, they rotate around the R axis instead. Then the R axis does not precess, so it can stay aligned with the magnetic field, so that the tetrahedra stay in $\mathcal{M}_q$. A qualitatively correct expression for this molecule is illustrated in Fig. 6.

The optimal size L_q of a composite vortex is determined by the competition between the anisotropy-induced confinement and the Coulomb repulsion one expects of like-signed vortices. The Zeeman cost is restricted to the composite core where the tetrahedra are tilted and may be estimated by replacing the total condensate size R in Eq. (8) by the molecule-size L. On the other hand, the elastic energy cost of rapid changes in the order parameter (the gradient term in the Hamiltonian) pushes the vortices apart. The tetrahedra along circles around the molecule rotate twice as far because the two vortices act in concert. This effect is described by the Coulomb energy (see Sec. IV B), $2\pi\frac{n_0\hbar^2}{m}\ln\frac{R}{L}+\pi\frac{n_0\hbar^2}{m}\ln\frac{L}{a_c}$, where m is the mass of the atoms in the condensate. The terms describe the energy outside and inside the molecule. The energy of the vortex molecule is therefore

$$E=k\frac{q^2L^2}{\beta}-\pi\frac{n_0\hbar^2}{m}\ln\frac{L}{a_c}+2\pi\frac{n_0\hbar^2}{m}\ln\frac{R}{a_c}, \tag{9}$$

where k is a numerical constant. The equilibrium size, determined by minimizing over L, is

$$L\sim L_q=\frac{\hbar}{q}\sqrt{\frac{n_0\beta}{m}}. \tag{10}$$

This vortex molecule is not "absolutely stable" (see Sec. V A). It has the same net rotation as three vortices each involving a rotation through 120° about the R axis. If the two vortices in the molecule *were* to coalesce in spite of their Coulomb repulsion, then they could react to form these three vortices, which have a lower energy and are not bound by the Zeeman effect. The vortex molecule of the two A rotations is *metastable* because thermal fluctuations can push them together, leading to such a fission process. The actual decay process is described in Sec. V D.

III. TOPOLOGICAL CHARGES

Vortices are simplest to understand when the space of all possible order parameters, the Hilbert space $\mathcal{H}$, has a single submanifold, $\mathcal{N}$, of ground states rather than a hierarchy of subspaces of lower and lower energies. Far away from any texture in the spin field, the order parameter lies in $\mathcal{N}$. Vor-

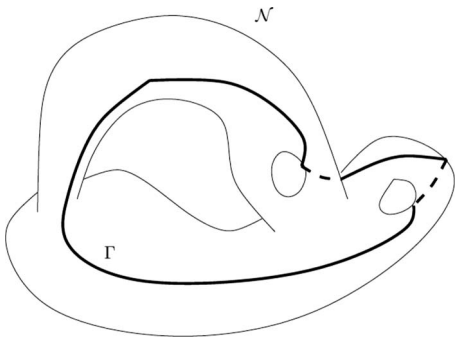

FIG. 3. The order parameter at infinity of a vortex winds around a loop Γ in the order-parameter space $\mathcal{N}$. (The space illustrated here is the surface of a solid with an arch and two openings which the order parameter passes through.) Realistic order-parameter spaces are usually more symmetrical.

tices are classified by the topology of the circuit $\psi(R\cos\phi, R\sin\phi)$ traced out in $\mathcal{N}$ by the order parameter on a large circle containing a vortex or set of vortices. Although there are many ways to add wiggles to a given circuit, only the circuit's topological structure is important, leading to a discrete set of possible vortex charges. Figure 3 shows how a circuit may be tangled with holes in the space $\mathcal{N}$. If the circuit describing the spin texture at infinity is tangled, the order parameter must leave $\mathcal{N}$ in at least one small region, the core of the vortex; to see this, imagine contracting the large circle in the condensate to a point; the corresponding circuit in order-parameter space cannot contract to a point without leaving $\mathcal{N}$.

Furthermore, as a field configuration evolves, the circuit describing the field on a large circle can evolve only into other circuits that are tangled in the same way; thus the vortex charge is conserved. This generalizes circulation conservation in a single-component condensate, such as helium 4. The sum of the quantum numbers of a set of ordinary vortices is equal to the number of times that the wave function at infinity winds around the circle that minimizes the Mexican hat potential.[49] For a multicomponent condensate, the tangling of a circuit can be described by a group of generalized winding numbers around the ground-state manifold $\mathcal{N}$, called the "fundamental group," or $\pi_1(\mathcal{N})$.

For a symmetric order-parameter space, the topological charge is the symmetry transformation that the order parameter undergoes as the vortex is encircled. Usually, all the ground states can be obtained by applying a symmetry σ to a reference state ψ_0. One can determine the topology of a set of vortices by traveling from $\phi=0$ to 2π around a loop λ enclosing them (λ is parameterized by ϕ, a variable ranging from 0 to 2π). Each local ground state along the loop can be expressed in the form

$$\psi(\phi) = D[\sigma(\phi)]\psi_0. \tag{11}$$

[The symmetry σ is taken from a group Σ with the same local structure as the more complicated group of $2F+1 \times 2F+1$ matrices describing the symmetries of the spinors. $D(\sigma)$ is the spin-$2F+1$ representation of σ.] One would like to use the ratio of $\sigma(2\pi)$ to $\sigma(0)$ to name the vortex, but there are multiple ways to choose σ because the ground state is symmetrical. However, after $\sigma(\phi)$ is chosen randomly at $\phi=0$, ambiguity can be avoided by making sure that $\sigma(\phi)$ changes gradually up to $\phi=2\pi$. When ϕ returns from 2π to 0 as the circuit closes, σ may jump. The order parameter itself is continuous, $D[\sigma(\phi=0)]\psi_0 = D[\sigma(\phi=2\pi)]\psi_0$, or

$$D(\sigma_\lambda)\psi_0 = \psi_0, \tag{12}$$

where σ_λ, the "magnitude" of the jump, is defined by

$$\sigma_\lambda = \sigma(0)^{-1}\sigma(2\pi). \tag{13}$$

Equation (12) shows that σ_λ is a symmetry of the ground-state wave function. When the ground state has a discrete symmetry group (as a tetrahedron has), σ_λ has only a discrete set of possible values, and so σ_λ is called the *topological charge* of the configuration. In order for these charges to completely classify the vortex topology, Σ must be a simply connected group.

Besides the conservation of topological charge, two further properties of vortices follow from the geometry of the internal ground-state space. First of all, the *net winding* or topological "charge" of a curve surrounding a set of vortices can be found by multiplying their individual charges together, where

$$\sigma_\lambda = \prod_i \sigma_i \tag{14}$$

is the change of the order parameter around a loop λ enclosing a cluster of vortices with individual charges σ_i. This rule is the generalization of adding the n's of ordinary vortices. (The fundamental group can be noncommutative so one has to multiply the charges together in the right order, see Appendix B.) Vortex alchemy is therefore constrained by the condition that such products do not change.

Second, the *kinetic energy* of a vortex can be estimated as a function of the winding behavior at infinity. Kinetic energy is the quantum-mechanical analog of elastic energy in a liquid crystal; since it is proportional to $|\nabla\psi|^2$, it measures the amount of variation of ψ on the large circle surrounding the vortices. To minimize the energy, the loop traced out by ψ in $\mathcal{N}$ therefore shrinks as much as is possible without leaving $\mathcal{N}$, becoming a *geodesic*. The energy of this most efficient vortex is related to the geodesic's length l by

$$E = \left(\frac{\hbar^2 n_0}{m}\ln\frac{R}{a_c}\right)\frac{l^2}{4\pi}, \tag{15}$$

where R and a_c are the radii of the condensate and the vortex core. (Note that replacing l by $2\pi n$ gives the standard expression for a vortex in a scalar condensate.)

A. Energy hierarchies and composite vortices

A small magnetic field introduces hierarchies into the order-parameter space, leading to spin textures, as illustrated in Fig. 1, that wind around one manifold at an intermediate length scale and around a smaller manifold far away. To describe this situation, it is useful to generalize the definition of a vortex core: a *core* is a region where the wave function

departs from any particular form. The black dots in Fig. 1 are one type of core (we call them the "component cores"); outside them the order parameter can be described by a generalization of the "phase-only" approximation[50]

$$\psi(x,y) \approx e^{-i\alpha(x,y)\hat{\mathbf{n}}(x,y)\cdot\mathbf{F}} e^{i\theta(x,y)} \sqrt{n_0}\chi_3. \tag{16}$$

These vortices would ordinarily be referred to as "coreless" because the *density* of the condensate does not drop to zero in them. In fact, if $\alpha \gg \beta$, the density is nearly uniform over the whole condensate. Vortices never force the density to vanish, as they do in an ordinary superfluid, because the space $\mathcal{S}$ of spinors satisfying $|\psi| = \sqrt{n_0}$ is a ten-dimensional sphere and does not have any necks for the order parameter to get looped around. However, the cores can still be identified by changes in the *magnetization*.[51]

The gray region in Fig. 1 is the "composite core," the region where the order parameter departs from the following form:

$$\psi(x,y) \approx e^{-i\alpha(x,y)F_z} e^{i\theta(x,y)} \sqrt{n_0}\chi_3. \tag{17}$$

The composite core can be identified by the changing orientation of the tetrahedra.

The energy scales corresponding to the order-parameter spaces $\mathcal{M}_q$, $\mathcal{M}$, and $\mathcal{H}$ are $V_{tot} - V_{\min} = 0$, $\epsilon(q) = \frac{q^2}{\beta}$ and βn_0^2 [see Eqs. (4) and (5) for the values of these energies; since $\beta \ll \alpha$, it sets the energy scale for the component cores]. The condensate can move out of the ground state into one of the higher-energy subspaces if forced to by topology, "spending less space" in the manifolds with the greater energies. (A temporal analog is saving gas by using a bicycle to get around town, but renting a car for trips to go see the autumn leaves in New Hampshire.) The size L_i of the ith nested core region, where ψ is in the space $\mathcal{M}_i$ with energy scale ϵ_i, turns out to be the same as the ith healing length, the distance over which the order parameter relaxes from $\mathcal{M}_i$ to the next lower-energy space. To estimate this length in terms of the energy scale ϵ_i, assume equipartition between kinetic and potential energies contained in the ith core so that ϵ_i is equal to $\frac{K}{L_i^2}$, a typical scale for the kinetic-energy density $\frac{\hbar^2}{2m}|\nabla\psi|^2$ at this level of the hierarchy (the superfluid stiffness, K, is $\frac{\hbar^2 n_0}{m}$). Hence, $L_i \sim \sqrt{\frac{K}{\epsilon_i}}$. This estimate gives the size of the composite vortex core

$$L_q \sim \sqrt{\frac{K\beta}{q^2}} \sim \frac{\hbar}{q}\sqrt{\frac{n_0\beta}{m}}, \tag{18}$$

as obtained in Eq. (10) by balancing forces between the individual component vortices. The component cores have typical diameters equal to the magnetic healing length

$$a_c \sim \sqrt{\frac{K}{n_0^2\beta}} \sim \hbar\sqrt{\frac{4\pi}{n_0\beta m}}. \tag{19}$$

Equations (16) and (17) imply that the charges of the component vortices are "tetrahedral charges" and the net charges of the composite vortices are "aligned charges." These can be classified based on the symmetry groups of $\mathcal{M}$ and $\mathcal{M}_q$, respectively. The symmetries of $\mathcal{M}$ and $\mathcal{M}_q$ can be parameterized by the simply-connected groups $\Sigma = G = \{(g,\theta)\,|\,g \in \mathrm{SU}_2 \text{ and } \theta \in \mathbb{R}\}$ and $\Sigma = G_q = \{(\alpha,\theta)\,|\,\alpha,\theta \in \mathbb{R}\}$, respectively,

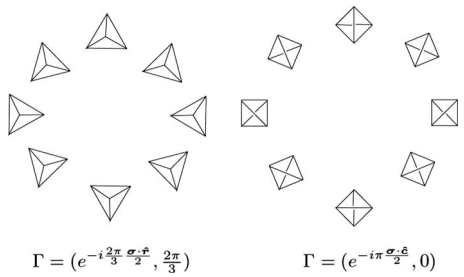

FIG. 4. Two tetrahedral vortices and their topological charges including the rotational and phase portions. The axes of the rotations, $\hat{\boldsymbol{r}}$, $\hat{\boldsymbol{c}}$, point along the symmetry axes of the tetrahedron which are labeled with R and C in Fig. 2. The first vortex is an aligned vortex if the magnetic field is perpendicular to the plane and $c > 4$.

$$D(e^{-i\alpha(\hat{\mathbf{n}}\cdot\boldsymbol{\sigma}/2)}, \theta) = e^{i\theta - i\alpha\hat{\mathbf{n}}\cdot\mathbf{F}} \tag{20}$$

$$D_q(\alpha,\theta) = e^{i\theta - i\alpha F_z}. \tag{21}$$

Both parameterizations are redundant—they ensure that the $\pm 2\pi$ phase vortices are assigned different charges even though both involve a net phase change $1 = e^{2\pi i}$. The vortex charges are defined by Eq. (11) and Eq. (13) with $\psi_0 = \sqrt{n_0}\chi_3$,

$$\Gamma_\lambda = (g_\lambda, \theta_\lambda) = (e^{-i\alpha_\lambda \hat{\mathbf{n}}_\lambda\cdot\boldsymbol{\sigma}/2, \theta_\lambda}) = (g(0)^{-1}g(2\pi), \theta(2\pi) - \theta(0)) \tag{22}$$

$$Q_\lambda = (\alpha_\lambda, \theta_\lambda)_3 = [\alpha(2\pi) - \alpha(0), \theta(2\pi) - \theta(0)]_3. \tag{23}$$

A tetrahedral charge is described by one of the 24 symmetries of the tetrahedron g_λ and a phase θ_λ; two examples are illustrated in Fig. 4. An aligned charge is described by the angle α_λ, of a rotation of the tetrahedron around the magnetic field direction, and a phase. The subscript 3 indicates that the tetrahedra rotate around a threefold symmetry axis (for $c > 4$).

We can now deduce, from Eq. (14), the formula which ensures that a cluster of tetrahedral vortices (charges Γ_i) can combine together to survive in a magnetic field, as a composite vortex with charge $Q_\lambda = (\alpha,\theta)_3$,

$$\prod_i g_i = e^{-i\alpha\sigma_z/2},$$

$$\sum_i \theta_i = \theta. \tag{24}$$

Now let us consider the form of the fields around tetrahedral vortex i. The spin texture will be rotationally symmetric

$$\psi = e^{i\theta_i/2\pi\phi} e^{-i\alpha_i/2\pi\phi\hat{\boldsymbol{n}}_i'\cdot\mathbf{F}}\sqrt{n_0}\chi_0, \tag{25}$$

where ϕ is now the azimuthal angle ϕ centered at this vortex and θ_i, α_i, and $\hat{\boldsymbol{n}}_i'$ are *constants*. Because the tetrahedra near this vortex may be tilted, we use $\sqrt{n_0}\chi_0$, a *generic* member of the cyclic order-parameter space. The axis $\hat{\boldsymbol{n}}_i'$ is a local symmetry axis for the *tilted* tetrahedra.

Now let us rewrite Eq. (25) in terms of χ_3. Let $\chi_0 = D(R,\xi)\chi_3$ for some rotation R and phase ξ and rewrite Eq. (25) as

$$\psi(\phi) = D(R,\xi)e^{i\theta_i/2\pi\phi}e^{-i\alpha_i/2\pi\phi\hat{\boldsymbol{n}}_i\cdot\mathbf{F}}\sqrt{n_0}\chi_3, \tag{26}$$

where

$$\hat{\boldsymbol{n}}_i = R^{-1}(\hat{\boldsymbol{n}}_i'). \tag{27}$$

We have used the transformation rule for angular momentum

$$D(R,\xi)^\dagger F^i D(R,\xi) = \sum_{j=1}^{3} R_{ij}F_j. \tag{28}$$

(R_{ij} is the 3×3 matrix describing the rotation in Cartesian coordinates.) Equation (26) expresses the vortex as a product of a constant matrix $D(R,\xi)$ (the phase ξ is unimportant) and a standardized vortex configuration. The transformation $D(R,\xi)$ rotates the standardized configuration in spin space, changing both the rotation axis (from $\hat{\boldsymbol{n}}_i$ to the local axis $\hat{\boldsymbol{n}}_i'$) and the orientation of the tetrahedra. The symmetry axis $\hat{\boldsymbol{n}}_i$ has one of the special orientations illustrated in Fig. 2(a) and the group element that classifies this vortex is $\Gamma_i = (e^{-i\alpha_i(\boldsymbol{\sigma}\cdot\hat{\boldsymbol{n}}_i/2)}, e^{i\theta_i})$. [Although Eq. (25) might seem to suggest that there is a continuous family of vortices, one for each $\hat{\boldsymbol{n}}_i'$, the topological charge is defined in terms of how $\sqrt{n_0}\chi_3$ transforms.]

B. Enumerating vortex charges

Let us start with the *tetrahedral* charges [see Eq. (22)], $\Gamma=(g,\theta)$. We will introduce a geometrical notation for the symmetries g of the tetrahedra, which are elements of SU_2. Surprisingly, SU_2 is necessary for classifying vortices even when one is dealing with integer spin particles. In SU_2, rotation angles are defined modulo 4π rather than 2π. Therefore any rotation can be described as a rotation through an angle α around some axis, where $-2\pi < \alpha \leq 2\pi$, and a negative angle refers to a clockwise rotation. The 12 symmetries of the tetrahedron according to the ordinary method of counting become 24. Ordinarily, one considers a clockwise 240° rotation around an axis to be the same as the counterclockwise 120° rotation. The corresponding SU_2 matrices, however, differ by a minus sign. This is more than a technical point: the corresponding vortices cannot deform into one another and in fact have different energies.

Let us describe g with reference to the tetrahedron in Fig. 2(a). We refer to the minimal rotation around a given axis using just the label of the axis; hence S,P,Q, and R refer to the rotations through 120° counterclockwise as viewed from the tips of the corresponding arrows and A,B, and C refer to counterclockwise rotations through 180° about A,B, and C. Rotations through larger angles can be written as powers of these rotations. Thus, $P^2=P^{-4}$ is a 240° rotation and $P^3 = A^2 = -id$.

Substituting $\sigma_\lambda = e^{i\theta}e^{-i\alpha\hat{\boldsymbol{n}}\cdot\mathbf{F}}$ into Eq. (12) gives a relationship between θ and g,[19,20] so the phases which may accompany a given rotational symmetry form an arithmetic sequence, $\theta_0+2\pi m$. (The value of θ_0 can be found geometrically, see Ref. 42.) Working out the value of θ_0 shows that an S,P,Q, or R rotation-vortex always involves a *fractional* phase shift of $\frac{2\pi}{3}$ plus a multiple of 2π, while the A,B, and C vortices do not have fractional phase shifts. Hence, the vortex types are $(\pm id, 2\pi m)$, $(R^n, \frac{2\pi n}{3}+2\pi m)$, and $(\pm A, 2\pi m)$, where $n=\pm 1,\pm 2$ and m is an integer, as well as the corresponding vortices with R replaced by P, Q, or S and A replaced by B or C.

One can work out explicit expressions for the SU(2) elements corresponding to given rotations. For example, let us find the SU(2) element corresponding to A; since the rotation angle is 180°,

$$A = e^{-i\pi(\hat{\boldsymbol{a}}\cdot\boldsymbol{\sigma}/2)} = -i\hat{\boldsymbol{a}}\cdot\boldsymbol{\sigma}, \tag{29}$$

where $\hat{\boldsymbol{a}}$ is the A axis. Note that the tetrahedron has its vertices at $(0,0,-1)$, $(-\frac{2\sqrt{2}}{3},0,\frac{1}{3})$, $(\frac{\sqrt{2}}{3},\sqrt{\frac{2}{3}},\frac{1}{3})$, and $(\frac{\sqrt{2}}{3},-\sqrt{\frac{2}{3}},\frac{1}{3})$. The A axis bisects the segment connecting the last pair of points; the midpoint of these two points is

$$\frac{1}{2}(\hat{\boldsymbol{p}}+\hat{\boldsymbol{q}}) = \left(\frac{\sqrt{2}}{3},0,\frac{1}{3}\right). \tag{30}$$

The unit vector $\hat{\boldsymbol{a}}$ is obtained by normalizing this vector, so

$$\hat{\boldsymbol{a}} = \left(\sqrt{\frac{2}{3}},0,\sqrt{\frac{1}{3}}\right). \tag{31}$$

Hence by Eq. (29),

$$A = -i\sqrt{\frac{2}{3}}\sigma_x - i\sqrt{\frac{1}{3}}\sigma_z. \tag{32}$$

The net charge of a set of vortices, Eq. (14), is found by adding their phases and multiplying the g matrices for the vortices of the set, identifying the result as one of the rotations A^n,B^n,P^n, etc. This procedure completely determines the SU(2) product element, whereas the geometric method of applying the appropriate sequence of rotations to a tetrahedron does not determine the *sign* of the SU(2) matrix.

We will describe a vortex reaction with the following notation:

$$(-id,0) \rightarrow \left(R,\frac{2\pi}{3}\right) * \left(R,\frac{2\pi}{3}\right) * \left(R,-\frac{4\pi}{3}\right). \tag{33}$$

The $*$ is a reminder that the products of the charges on both sides have to be equal.

Another useful cyclic spinor is

$$\chi_2 = \begin{pmatrix} \frac{1}{2} \\ 0 \\ -\frac{i}{\sqrt{2}} \\ 0 \\ \frac{1}{2} \end{pmatrix}. \tag{34}$$

This spinor corresponds to the tetrahedron in Fig. 2(b). Its vertices are at the points of the form $(\pm\frac{1}{\sqrt{3}},\pm\frac{1}{\sqrt{3}},\pm\frac{1}{\sqrt{3}})$ if we restrict the choices of signs so that there are always 0 or 2 minus signs. The A, B, and C axes of the tetrahedron are aligned with the x, y, and z coordinate vectors. These simple axes make this orientation more convenient for working out

the charge matrices and checking tetrahedral charge conservation. [For example, $\hat{\boldsymbol{p}}=(\frac{1}{\sqrt{3}},-\frac{1}{\sqrt{3}},-\frac{1}{\sqrt{3}})$, since vertex P is in the $x>0,y<0,z<0$ octant. Thus $P=e^{-i(\pi/3)\hat{\boldsymbol{p}}\cdot\boldsymbol{\sigma}}=(1-i\sigma_x+i\sigma_y+i\sigma_z)/2$.]

When $c>4$, the ground-state space is $\mathcal{M}_{q3}$. Vortices are described as in Eq. (23) by an ordered pair $(\alpha,\theta)_3$, with the subscript 3 indicating that this phase has order-3 symmetry. The continuity of the wave function's phase limits the vortex types to the form

$$Q=(\alpha,\theta)_3=\left(\frac{2\pi m}{3},2\pi\left(\frac{m}{3}+n\right)\right)_3. \tag{35}$$

According to Eq. (24), the component vortices' charges (g_i,θ_i) in a molecule of this net charge must satisfy

$$\prod_i g_i=R^m,$$

$$\sum_i \theta_i=2\pi\left(\frac{m}{3}+n\right). \tag{36}$$

When $c<4$, minimizing Eq. (5) implies that the magnetic field axis is an order-2 symmetry and the ground-state space is $\mathcal{M}_{q2}$, the rephasings and rotations about z of $\sqrt{n_0}\chi_2$. Now $(\alpha,\theta)_2$ specifies the vortex types. The possibilities are

$$Q=(\alpha,\theta)_2=(\pi m,2\pi n)_2. \tag{37}$$

The relation between Q and its component tetrahedral vortices is similar to Eq. (36), with C appearing instead of R.

IV. ENERGIES AND SYMMETRIES

This section continues the analysis of the energy function Eq. (3) by considering the effects of the magnetic field and the kinetic energy on the energy of textures.

A. Anisotropy potential

The orientation of the tetrahedron that is preferred by a magnetic field along the z axis is determined by an effective potential, a function of the orientation of the tetrahedron. As long as

$$q\ll n_0\beta, \tag{38}$$

the tetrahedron will be only slightly deformed as it rotates. This deformation is described by a space $\mathcal{M}'$ displaced by a distance on the order of $\frac{q}{n_0\beta}$ from the space $\mathcal{M}$ of perfect tetrahedra. The spinors in the distorted space are given by

$$\psi=\sqrt{n_0}D(R,\xi)\chi_2+\delta\psi, \tag{39}$$

where $D(R,\xi)$ is the spin-2 rotation matrix corresponding to the rotation R of space multiplied by a phase. The distortion $\delta\psi$ depends on the orientation R. Equation (16) does not explicitly mention this distortion for convenience. In this section, we use $\sqrt{n_0}\chi_2$ as the standard spinor orientation instead of $\sqrt{n_0}\chi_3$ to simplify calculating the energy; conveniently, the body axes A,B, and C of the corresponding tetrahedron for the *former* state are aligned with the coordinate axes $\hat{\mathbf{x}},\hat{\mathbf{y}}$, and $\hat{\mathbf{z}}$. The body axes of the rotated state $D(R)\sqrt{n_0}\chi_2$ (which make the angles α_1,α_2, and α_3 with the z axis) are thus $R(\hat{\mathbf{x}}),R(\hat{\mathbf{y}})$, and $R(\hat{\mathbf{z}})$. Therefore the z component of the spin, in terms of the components of the spin along the body axes, is

$$D(R)^\dagger F_z D(R)=\cos\alpha_1 F_x+\cos\alpha_2 F_y+\cos\alpha_3 F_z. \tag{40}$$

This expression can be understood by taking the inner product between the spin, (F_x,F_y,F_z) in the body coordinates and the $\hat{\boldsymbol{z}}$ vector whose body coordinates are $(\cos\alpha_1,\cos\alpha_2,\cos\alpha_3)$,

At first order the quadratic Zeeman effect does not have any dependence on the orientation of the tetrahedron because a cyclic spinor is "pseudoisotropic," i.e., $\chi_2^\dagger F_i F_j\chi_2=2\delta_{ij}$. The first-order energy is thus given by

$$\begin{aligned}\langle qF_z^2\rangle &\approx n_0 q\chi_2^\dagger D(R)^\dagger F_z^2 D(R)\chi_2\\ &\approx n_0 q\sum_{i,j=1}^{3}\cos\alpha_i\cos\alpha_j\chi_2^\dagger F_i F_j\chi_2\approx 2n_0 q,\end{aligned} \tag{41}$$

which does not prefer any orientation of the tetrahedron. In the last step we used

$$\sum_{i=1}^{3}\cos^2\alpha_i=1, \tag{42}$$

which follows from the fact that $\hat{\boldsymbol{z}}$, a unit vector, has body coordinates $(\cos\alpha_1,\cos\alpha_2,\cos\alpha_3)$.

To find the second-order energy due to the quadratic Zeeman effect, which will break the tie, we have to find the deformed state and its energy. The deformation $\delta\psi$ is determined by minimizing the total interaction and Zeeman energy in Eq. (4) for each given orientation R. Now if the deformation is not restricted somehow, the "deformation" which minimizes the energy will be very large, involving the tetrahedron rotating all the way to the absolute ground state. We therefore allow only deformations of the form

$$\begin{aligned}\delta\psi=dD(R,\xi)\chi_2+\frac{1}{\sqrt{2}}(aD(R,\xi)F_x\chi_2+bD(R,\xi)F_y\chi_2\\ +cD(R,\xi)F_z\chi_2)+(e+if)D(R,\xi)\chi_{2t},\end{aligned} \tag{43}$$

where a,b,c,d,e, and f are real numbers. (These terms correspond to the excitation modes of the cyclic state presented in Ref. 52) This correction only perturbs ψ in six of the ten directions in the Hilbert space. The other four directions are accounted for by the rotation R and the phase ξ which would be Goldstone modes when $q=0$. (Of course, the energy remains ξ independent even when $q\neq 0$.) The particular six stiff deformations in Eq. (43) are chosen because they are orthogonal to infinitesimal rotations and rephasings of the tetrahedral state. We have to find the deformations that minimize V_{tot}, Eq. (4), for each rotation R.

To evaluate V_{tot}, note that $D(R,\xi)$ cancels from all the terms in the energy except for the Zeeman term, where one can use Eq. (40). The resulting expression for the energy density reads

$$V_{tot}(\psi) = \frac{1}{2}\alpha(\tilde{\psi}^\dagger\tilde{\psi})^2 + \frac{1}{2}\beta(\tilde{\psi}^\dagger\mathbf{F}\tilde{\psi})^2 + \frac{1}{2}\gamma|\tilde{\psi}_t^\dagger\tilde{\psi}|^2 - \mu\tilde{\psi}^\dagger\tilde{\psi} - q\sum_{i,j=1}^{3}\cos\alpha_i\cos\alpha_j\tilde{\psi}^\dagger F_i F_j\tilde{\psi}, \quad (44)$$

where $\tilde{\psi}=\sqrt{n_0}\chi_2+d\chi_2+\frac{1}{\sqrt{2}}(aF_x\chi_2+bF_y\chi_2+cF_z\chi_2)]+(e+if)\chi_{2t}$ is the perturbed wave function without the rotation. (Working with $\tilde{\psi}$ is equivalent to fixing the orientation of the tetrahedron and rotating the magnetic field.) The effective potential Eq. (5) is obtained by minimizing V_{tot} over $a,b,\ldots$ while keeping R fixed. Some details of this minimization are in Appendix A.

The effective potential justifies regarding L_q as a type of healing length, the "tetrahedron tipping length:" when the tetrahedra are rotated out of the appropriate ground-state orientation at the edge of a condensate, the competition between the kinetic energy and the anisotropy energy, by Eq. (5), encourages the order parameter to return to $\mathcal{M}_q$ within the distance $L_q\sim\frac{\hbar}{q}\sqrt{\frac{n_0\beta}{m}}$.

Now the ground states can be found as a function of c. When $c>4$, a short calculation shows that Eq. (5) has its minimum at $\cos\alpha_i=\pm\frac{1}{\sqrt{3}}$, $i=1,2,3$; i.e., when the magnetic field is along the line connecting a vertex of the tetrahedron to the opposite face or vertex. Hence the order-parameter space $\mathcal{M}_q$ is as given in Eq. (17). When $c<4$, the effective potential is minimized by taking $(\cos\alpha_1,\cos\alpha_2,\cos\alpha_3)=(\pm1,0,0)$ (or some permutations); i.e., one of the lines joining an opposite pair of edges of the tetrahedron should be parallel to the magnetic field (see Fig. 2).

For $c>4$, the tetrahedron can point either along or opposite to the magnetic field, breaking time-reversal symmetry spontaneously. In fact, Appendix A shows that these ground states are ferromagnetic—they have small magnetizations pointing in the direction opposite the apex of the tetrahedron (either parallel or antiparallel to the magnetic field). The symmetry breaking is spontaneous because the *quadratic* Zeeman term is time-reversal invariant.[53] The appearance of the magnetization for $c>4$ can be understood intuitively using the geometrical representation of Ref. 41. When a magnetic field is applied along the z axis, the tetrahedron representing a cyclic state is compressed toward the xy plane; moving the spin nodes away from the north and south poles increases the probability that $F_z=\pm2$ (see Ref. 41) and thus decreases the quadratic Zeeman energy. In particular, the base of the tetrahedron illustrated in Fig. 2(a) gets pushed toward the vertex at $-\hat{z}$. This distorted tetrahedron has a nonzero magnetization.

We can also understand intuitively the transition as c decreases by comparing the distortion just described to the distortion of Fig. 2(b). Compressing this tetrahedron pushes its upper and lower edges together, toward the xy plane. In a perfect tetrahedral state, $\mathbf{m}=\psi^\dagger\mathbf{F}\psi=0$ and $\theta=\psi_t^\dagger\psi=0$, minimizing the interaction energies in Eq. (4). On the other hand, when $q\neq0$, the compressed version of Fig. 2(a) has a nonzero magnetization while the compressed version of Fig. 2(b) is symmetric between $\pm z$ and therefore has zero magnetization but has a nonzero θ. Therefore the orientation of the ground-state tetrahedron is determined by whether $\boldsymbol{m}^2$ or $|\theta|^2$ is the more important term in the Hamiltonian.

The main source of anisotropy is different at sufficiently low magnetic fields;[33] the cubic Zeeman effect, proportional to B^3, then dominates over the effective potential in Eq. (5), proportional to B^4. Nevertheless B can be increased enough for the order B^4 effect we have calculated to dominate over the B^3 effect without invalidating the perturbation theory just described. This is possible because the denominator $n_0\beta$ in Eq. (5) is small compared to the hyperfine energy splitting A_{HF}. For spin-2 atoms the effect of the magnetic field is given by

$$V_{nz} = \psi^\dagger\sqrt{(\mu_B B)^2 + A_{HF}^2 + A_{HF}\mu_B B F_z}\psi, \quad (45)$$

where A_{HF} is the hyperfine coupling. It follows that the quadratic and cubic Zeeman effects are $qF_z^2=\frac{\mu_B^2B^2}{8A}F_z^2$ and $\frac{\mu_B^3B^3}{16A^2}F_z^3$. The analysis we have given applies when the magnetic field is weak enough that the wave function is not drastically distorted, Eq. (38), but strong enough for the second-order effect of the quadratic Zeeman term to dominate over the cubic Zeeman term. These conditions combine into

$$n_0\beta \ll \mu_B B \ll \sqrt{A_{HF}n_0\beta}. \quad (46)$$

For ^{87}Rb at density $5\times10^{20}/m^3$, $n_0\beta=3$ nK and $A_{HF}=160$ mK while $\mu_B=67$ μK/Gauss; hence the anisotropy potential used here is actually valid for a wide range of magnetic fields—between 0.04 mG and 0.3 G.

B. Kinetic energy and the energy index

The interaction between scalar vortices, which arises because the kinetic energy in their superflow depends on the distance between them, takes the form of a two-dimensional Coulomb interaction[54] which is proportional to $n_1n_2\ln r_{12}$, where n_1 and n_2 are the circulation quantum numbers and r_{12} is the distance between the vortices. For noncommutative vortices in a phase with more symmetry, the leading behavior of the interaction is similar, depending on topological charges, Eq. (22), and varying logarithmically with the distance between vortices.

Consider an isolated vortex first. Since the interaction energy V_{tot} is constant (and equal to its minimum) at infinity, kinetic energy determines the form of the vortex at great distances. In order for the kinetic energy to be minimal, the field on a circle around it should trace out a geodesic, as mentioned above. To see this suppose the vortex is given far away by the radius-independent expression

$$\psi(r,\phi) = \sqrt{n_0}F(\phi) \quad (47)$$

for an appropriate spinor function $F(\phi)$. The kinetic energy outside the core of radius a_c is

$$E \approx \int\int d^2\mathbf{r}\frac{\hbar^2}{2m}\nabla\psi^\dagger\nabla\psi$$
$$\approx \int_0^{2\pi} n_0|F'(\phi)|^2 d\phi \int_{a_c}^{R}\frac{\hbar^2}{2mr^2}rdr$$
$$\approx \frac{\hbar^2 n_0}{2m}\ln\frac{R}{a_c}\int_0^{2\pi}|F'(\phi)|^2 d\phi. \quad (48)$$

Now the curve parameterized by $F(\phi)$ adjusts itself so as to minimize the last integral, while maintaining the topology of the circuit traced out by $F(\phi)$ in the order-parameter space. One can show that an integral of this form is minimized when $F(\phi)$ traces out a closed *geodesic* in the ground-state space. The length of a closed curve is defined by $\int_0^{2\pi}|F'(\phi)|d\phi$, so it is not surprising that the geodesic of charge Γ, which minimizes this expression, also minimizes Eq. (48).[55] Furthermore, if the geodesic has length l_Γ, then $\int_0^{2\pi}d\phi|F'(\phi)|^2=\frac{l_\Gamma^2}{2\pi}$.

The cyclic order-parameter space can be obtained from a perfect sphere in four dimensions by tiling this sphere with 24 identical regions and identifying corresponding points (just as one constructs a torus from a periodically tiled crystal). The *closed* geodesics of the cyclic order-parameter space are represented by arcs of great circles connecting *corresponding* points. Great circles are described by Eq. (25). Hence in the field of a minimum-energy vortex, the tetrahedra rotate at a fixed rate around a single axis. (For a shape less isotropic than a tetrahedron, the order parameter would rotate around a wobbling axis according to Euler's rigid-rotation equations.) Substituting the symmetrical $F(\phi)$ into Eq. (48) gives[50]

$$E \approx \frac{\hbar^2 n_0}{2m}\ln\frac{R}{a_c}\int d\phi\psi^\dagger\left(-\alpha\frac{\hat{\mathbf{n}}\cdot\mathbf{F}}{2\pi}+\frac{\theta}{2\pi}\right)^2\psi$$
$$\approx \frac{\hbar^2 n_0}{4\pi m}\ln\frac{R}{a_c}\left[\alpha^2\left(n_i n_j Q_{ij}+\frac{s(s+1)}{3}\right)-2\alpha\theta n_i M_i+\theta^2\right], \quad (49)$$

where the general expression for any spin s and any phase has been given in terms of the quantum fluctuation matrix $Q_{ij}=\frac{1}{n_0}(\psi^\dagger\frac{F_iF_j+F_jF_i}{2}\psi)-\frac{s(s+1)}{3}\delta_{ij}$ and the magnetization per particle $M_i=\frac{m_i}{n_0}$. The spin-2 tetrahedron state appears to be isotropic as long as one does not go beyond second-order correlators, as seen from the following calculations:

$$\langle\chi_3|F_i|\chi_3\rangle=0, \quad (50)$$

$$\langle\chi_3|F_iF_j|\chi_3\rangle=2\delta_{ij}, \quad (51)$$

and hence $M=Q=0$. Equation (49) implies that the energy is proportional to $l_\Gamma^2=(\theta^2+2\alpha^2)$, a generalization of the Pythagorean theorem showing how to combine the amount of rephasing and rotation to get the total geodesic length. A spin rotation costs twice as much energy as a rephasing by the same angle.

In order to study vortex stability and Coulomb forces, let us define the "energy index,"

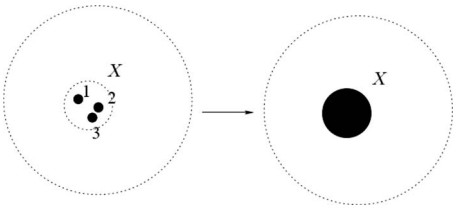

FIG. 5. A group of vortices is combined into the core of a composite vortex X. The energy outside the blacked-out core is calculated from the resultant winding number of the vortices inside and the energy inside the core is calculated by looking inside the core to see which vortices are actually there.

$$I_E=\left(\frac{l_\Gamma}{2\pi}\right)^2=\left(\frac{\theta}{2\pi}\right)^2+2\left(\frac{\alpha}{2\pi}\right)^2, \quad (52)$$

which is a fraction for each tetrahedral charge from Sec. III B. The energy of a vortex is given as $\frac{\pi\hbar^2 n_0}{m}\ln\frac{R}{a_c}I_E(\Gamma)$, a multiple of the energy of an ordinary phase vortex. The force between a pair of vortices can be expressed very simply in terms of I_E.

The force follows from an estimate of the energy of a cluster of vortices. Using ideas from Ref. 56, we think of the cluster as forming the "core" of a bigger vortex, as illustrated in Fig. 5. (We are not necessarily assuming that the vortices are bound together.) Draw a circle of radius X just around the group of vortices. The kinetic energy can then be found as the sum of the energies outside and inside of X; for the case illustrated in the figure this energy is approximately

$$\pi\frac{n_0\hbar^2}{m}\left(\left[I_E(X)\ln\frac{R}{L_X}\right]+\left\{[I_E(1)+I_E(2)+I_E(3)]\ln\frac{L_X}{a_c}\right\}\right), \quad (53)$$

where L_X is the diameter of the group being combined together and R is the radius of whole system. The first term describes the energy outside of X. Sufficiently far outside of X, the field should have the form of a rotationally symmetric vortex. Hence the energy outside X is given by an expression such as in Eq. (49), except that a_c must be replaced by L_X. The energy inside X is approximated by adding the energies of the three vortices in it, which are calculated such as in Eq. (49) but now with R replaced by L_X.

The general expression for the energy of a set of vortices with charges Γ_i, after rearranging the formula to emphasize the dependence on the diameter of the set L, is

$$E_K \approx \frac{\hbar^2\pi n_0}{m}\left[\sum_i I_E(\Gamma_i)-I_E\left(\prod_i\Gamma_i\right)\right]\ln\frac{L}{a_c}$$
$$+\frac{\hbar^2\pi n_0}{m}I_E\left(\prod_i\Gamma_i\right)\ln\frac{R}{a_c}. \quad (54)$$

The error resulting from ignoring the overlaps between the vortices' fields can be estimated if we assume that $q=0$. In this case, the only form of energy outside the vortex cores is the kinetic energy which has a symmetry under rescaling. Therefore (as pointed out in Ref. 56), the difference between Eq. (54) and the actual energy has the form

$$\Delta E = \frac{\pi n_0 \hbar^2}{m} f\left(\frac{L_{13}}{L_{12}}, \frac{L_{14}}{L_{12}}, \frac{L_{23}}{L_{12}}, \ldots\right) + O\left(\frac{a_c}{L}\right), \tag{55}$$

where the L_{ij}'s refer to the distances between pairs of vortices. This correction can be ignored relative to the order $\ln\frac{L}{a_c}$ terms kept in Eq. (53) *as long as the vortex spacings all have the same order of magnitude*, since in this case f has no singularity. The function f depends on the details of how the vortex textures are spliced together.

When there are just two vortices, the force between them can be calculated by differentiating Eq. (54), giving $-\frac{\hbar^2 \pi n_0}{mL}[I_E(\Gamma_1)+I_E(\Gamma_2)-I_E(\Gamma_1\Gamma_2)]$. This is *exact* (if $L \gg a_c$ and $q=0$) since for two vortices, the error in the energy, Eq. (55), has to be a constant.[57] For any number of vortices, Eq. (54) shows that $\frac{dE}{dL}$ is negative or positive, or equivalently, the vortices repel or attract each other, accordingly as the index of the combined vortex is greater or less than the sum of the separate vortices' indices.

Unlike the Coulomb interaction between vortices in an ordinary scalar superfluid, the interaction energy cannot be written as a sum of two-vortex interaction terms.[58] In fact, just knowing that any two vortices of a subset *repel* one another does not guarantee that they do not *collectively* attract one another. An example is the set of three $(A,0)$ vortices of index $\frac{1}{2}$. Two of them together make the vortex $(-id,0)$ of index 2 while all three of them combine into $(-A,0)$ of index $\frac{1}{2}$. Appendix B describes additional strange effects because of the charge multiplication being noncommutative.

V. CHEMISTRY OF VORTICES

In this section we will first discuss stability of isolated tetrahedral vortices and then determine when these vortices can combine to form molecules (and what the spin texture around a molecule looks like). Some of these molecules are only metastable and can each break up in several ways.

Briefly, bound states of vortices can form from stable tetrahedral vortices. As shown in Sec. V A, these are the vortices based on 120° symmetries of a tetrahedron, accompanied by a phase shift of $\frac{2\pi}{3}$ or $-\frac{4\pi}{3}$, and vortices based on 180° symmetries without a phase shift. Vortices with larger rotations or phase shifts will not occur as components of molecules. The net charge of the bound state must be field aligned.

A. Stable tetrahedral vortices

Only *stable* tetrahedral vortices will be found in the core region of composite vortices. A vortex of charge Γ is stable if there is a restoring force when Γ is forced to break up into the fragments Γ_i. The energy of the fragments can be found by substituting from Eq. (52) into Eq. (54) and increases with L only if $\Sigma_i(\theta_i^2+2\alpha_i^2) > (\theta^2+2\alpha^2)$. Therefore a vortex is absolutely stable if

$$\sum_i \left(\frac{\theta_i}{2\pi}\right)^2 + 2\left(\frac{\alpha_i}{2\pi}\right)^2 > \left(\frac{\theta}{2\pi}\right)^2 + 2\left(\frac{\alpha}{2\pi}\right)^2,$$

for *every* set of $\Gamma_i=(e^{-i(\alpha_i \sigma\cdot\hat{\mathbf{n}}_i/2)}, e^{i\theta_i})$ such that

$$\prod_i \Gamma_i = \Gamma. \tag{56}$$

We call this criterion *absolute* stability because it ensures that there are *no* lower energy states the vortex could decay to. Even if such states exist, there may be barriers which prevent the vortex from breaking up spontaneously, but let us assume for simplicity that such barriers do not exist for tetrahedral vortices. (We will show that analogous barriers do exist for *composite vortices*, whose core structure we can understand more easily.)

Let us now find all the stable vortices. The result will be that the one-third circulation vortex and the currentless vortex

$$\left(R, \frac{2\pi}{3}\right),$$

$$(C,0), \tag{57}$$

as well as their inverses and conjugates, are stable. Besides these,

$$\left(R, -\frac{4\pi}{3}\right),$$

$$(2\pi,0) \tag{58}$$

might be stable. The former [which is obtained by subtracting a phase of 2π from $(R,\frac{2\pi}{3})$] is more likely to be stable than the latter. To obtain this result we must find ways for all the other vortices to break up. For example, the vortex $(id,4\pi)$ can break up into two $(id,2\pi)$'s, halving the energy. We can generalize this example to infinitely many cases: any vortex with charge (g,θ) whose circulation θ is bigger than 2π can break up into $(g,\theta-2\pi)$ and $(0,2\pi)$ since $\theta^2 > (2\pi)^2+(\theta-2\pi)^2$. This leaves only finitely many vortices: the ones with phase-winding numbers not more than 2π. Aside from the vortices listed in Eq. (57) (and their inverses and conjugates), all the remaining vortices can break up as well. Their decay processes can be found by trial and error by multiplying together different combinations of tetrahedral charges until one finds a charge-conserving decay:

(1) $(-id,0)$ can break up into $(C,0)*(C,0)$ or $(R,2\pi/3)*(R,2\pi/3)*(R,-4\pi/3)$.

(2) $(-id,2\pi) \rightarrow (R,\frac{2\pi}{3})*(R,\frac{2\pi}{3})*(R,\frac{2\pi}{3})$.

(3) $(R^2,4\pi/3)$ can break up into $(R,2\pi/3)*(R,2\pi/3)$ and also $(S^{-1},4\pi/3)*(C,0)$.

(4) $(R^2,-2\pi/3) \rightarrow (S^{-1},-\frac{2\pi}{3})*(C,0)$.

(5) $(C,2\pi) \rightarrow (R,\frac{2\pi}{3})*(S^{-1},\frac{4\pi}{3})$.

(6) $(0,2\pi)$ has the same charge as $(R,\frac{2\pi}{3})*(R^{-1},\frac{4\pi}{3})$.

(7) $(R,-\frac{4\pi}{3})$ has the same charge as $(P^{-1},-\frac{2\pi}{3})*(Q^{-1},-\frac{2\pi}{3})$.

Breakups 1–5 lower the energy index and therefore lower the total energy by a logarithmically growing amount. On the

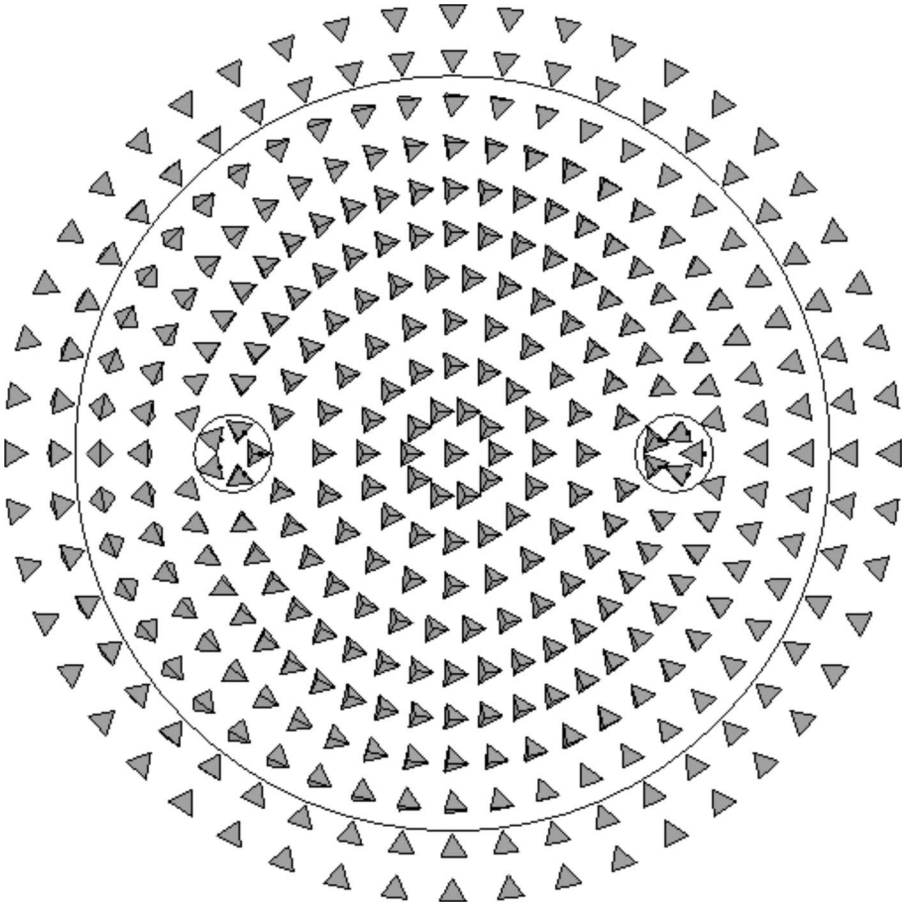

FIG. 6. An illustration of the composite vortex $(A,0)*(A,0)$. The magnetic field is perpendicular to the figure, so the tetrahedra prefer to be oriented with a face or a vertex facing up (since $c>4$). The two small circles enclose the 180° vortices, with symmetry axes indicated by black dots. Large circle indicates the transition region where the axis of the 360° rotation changes relative to the tetrahedra, from the A to the R axis. The figure uses a functional form with a rapid jump for $\mu(r)$ [unlike in Eq. (64)] for simplicity, so that the transition region does not overlap the cores. For the probably more realistic form given by Eq. (64), the tetrahedra are already tipped at the centers of the vortices so that the local rotation axes $\hat{\boldsymbol{n}}_i'$ do not have the standard orientations illustrated in Fig. 2(a).

other hand, the stability of the two vortices in Eq. (58) is unclear. Breakups 6 and 7 may either increase or decrease the energy, since they do not change the *energy index* and hence the remainder term in Eq. (54) needs to be taken into account. The vortex $(0,2\pi)$ is probably unstable if $\alpha \gg \beta$ because a pure phase vortex has to have an empty core (with energy density of order αn_0^2), while the two fragments it would break up into just have noncyclic cores (energy of order βn_0^2).[59] Whether $(R,-\frac{4\pi}{3})$ is stable or not we do not guess and the answer may depend on c.

B. Vortex molecules at $q \neq 0$ and their spin textures

In this section we will describe a qualitative wave function for the first example in Table I to improve on the schematic Fig. 1. Equation (36) states that a "molecule" made of the Γ_i's has an aligned charge; therefore it will not be expelled by the condensate. In particular, the example molecule has $\Gamma_1=\Gamma_2=(A,0)$ and $Q=(2\pi,0)_3$. Equation (36) follows by checking that $A=e^{-i(\pi/2\sqrt{3})(\sqrt{2}\sigma_x+\sigma_z)}$ and $A^2=-id$.

Writing a wave function that describes this example even qualitatively is a little more complicated than this simple calculation suggests. Just juxtaposing two A vortices next to one another gives a configuration which still has a large energy because the tetrahedra rotate 360° at infinity around the A axis instead of the R axis. A possible wave function without this shortcoming is illustrated in Fig. 6. We can build this wave function up in stages.

The straightforward juxtaposition is described by

$$\psi_{misalign} = e^{-i/2(\phi_1+\phi_2)(\sqrt{2/3}F_x+(1/\sqrt{3})F_z)}\sqrt{n_0}\chi_3, \tag{59}$$

where $\phi_i=\arctan\frac{y-y_i}{x-x_i}$ is the polar angle measured with respect to the location $(x_i,y_i)=\pm(\frac{L}{2},0)$ of the ith vortex. *This* wave function takes the form $\psi \approx e^{-i\phi(1/\sqrt{3})(\sqrt{2}F_x+F_z)}\sqrt{n_0}\chi_3$ at infinity where ϕ_1 and ϕ_2 approach ϕ. The tetrahedra rotate around a tilted axis, so they do not stay aligned appropriately with the magnetic field except on the x axis and the y axis (where the tetrahedra are reversed, but this is still a ground state). Another attempt, which uses the R axis instead of the A axis to eliminate the tilting of the tetrahedra,

$$\psi_{discontinuous} = e^{-i/2(\phi_1+\phi_2)F_z}\sqrt{n_0}\chi_3, \tag{60}$$

is a complete fiasco, since this function is not continuous along the line connecting the two cores. (The R axis has the

wrong symmetry, so as (x,y) circles around (x_2,y_2); $\psi_{discontinuous}$ changes from χ_3 to $e^{-i\pi F_z}\chi_3 \neq \chi_3$.) A hybrid of Eqs. (59) and (60), illustrated in Fig. 6, has neither of these problems,

$$\psi = e^{-i\phi[F_x \sin\mu(r)+F_z\cos\mu(r)]} \times e^{i\phi(\sqrt{2}F_x+F_z)/\sqrt{3}} e^{-i/2(\phi_1+\phi_2)\left[\sqrt{\frac{2}{3}}F_x+(1/\sqrt{3})F_z\right]}\sqrt{n_0}\chi_3, \tag{61}$$

where $\mu(r)$ must satisfy

$$\mu(0) = \arccos\sqrt{\frac{1}{3}}, \tag{62}$$

$$\mu(\infty) = 0. \tag{63}$$

For example, we could define

$$\cos\mu(r) = \sqrt{\frac{r^2+D^2}{r^2+3D^2}}, \tag{64}$$

where D can be used as a variational parameter.

Figure 6 illustrates this wave function. Note that the tetrahedra within the large circle have a texture similar to the one described by the initial guess; the tetrahedra 3 rows in from this circle as they rotate through 360° about the order-2 axis bisecting their right edge, producing all sorts of arbitrary orientations. The 360° axis changes from the A axis to the R axis as one crosses through the transition region indicated by the large circle. As you follow a radius outward past the circle, the tetrahedra are tipped by appropriate amounts and end up being aligned with the magnetic field. Indeed, the first two factors fix the field up at infinity by applying a continuously varying rotation to the overall texture. These factors change the axis from A to R at large r as one can see by replacing $\phi_1 \approx \phi_2$ by ϕ and using Eq. (63). (The amount of tipping required depends on ϕ; the tetrahedra on the negative x axis have to be tipped the most, though their original orientation is compatible with the magnetic field. The face which is on top is changed. This reorientation is required to make the amount of tipping continuous: the tipping angle increases more and more as ϕ goes from 0 to π.)

The two extra factors also do not produce any singularities. Although they seem to have a vortexlike discontinuity at the origin, the discontinuity cancels on account of Eq. (62). Near $(\pm\frac{D}{2},0)$, the texture *does* have vortices, of the form described by Eq. (26), where the tetrahedra are rotated around a tilted axis. Since the tetrahedra are tilted so that this axis lines up with their axis of symmetry, there is no branch singularity. For example, near vortex 2,

$$\psi \approx e^{-i\pi[F_x \sin\mu(L/2)+F_z\cos\mu(L/2)]} e^{-(i\phi_2+i\pi/2)(\sqrt{2/3}F_x+\sqrt{1/3}F_z)}\sqrt{n_0}\chi_3. \tag{65}$$

[According to Eq. (28), the local symmetry axis $\hat{\boldsymbol{n}}'$ is the rotation of the standard axis $\sqrt{\frac{2}{3}}\hat{\boldsymbol{x}}+\sqrt{\frac{1}{3}}\hat{\boldsymbol{y}}$ through a half-turn about $\hat{\boldsymbol{x}}\sin\mu(\frac{L}{2})+\hat{\boldsymbol{y}}\cos\mu(\frac{L}{2})$.]

In short, though $(A,0)^2=(-id,0)$, the cancellation of the Zeeman energy at infinity is not automatic. The topological classification just implies that the field in Eq. (59) *can* be deformed so that it aligns with the magnetic field at infinity, but does not say how to do it.

The kinetic energy of this composite vortex, according to Eq. (54), is

$$E_K \approx \frac{\hbar^2\pi n_0}{m}\{2I_E[(A,0)] - I_E[(-id,0)]\}\ln\frac{L}{a_c} + \frac{\pi\hbar^2 n_0}{m} I_E[(-id,0)]\ln\frac{R}{a_c}. \tag{66}$$

Adding the Zeeman energy now gives Eq. (9), except that k depends on the ratio of D and L, which can be optimized over for greater accuracy. The optimal scale for L is of order L_q [see Eq. (10)]. The equilibrium vortex separation is thus equal to the healing length for the orientation of tetrahedra, just as the core size of a spin vortex in a spin-1 condensate is equal to the magnetic healing length. In contrast, if a pair of tetrahedral vortices is stretched beyond the orientation-healing length, a "cord" of tipped tetrahedra of width L_q forms between them—a simple version of the string imagined to hold the quarks together in a rapidly rotating baryon. Vortex molecules of the type described here do not have this kind of stretched structure in equilibrium, since the Coulomb force cannot push them apart farther than a distance of L_q. (Smaller molecules occur when the component vortices have a short-range repulsion as in examples 6 and 7 of Sec. V A.)

The total energy of the molecule can be found by substituting L_q into Eq. (9) and using Eq. (19),

$$E_{\text{vortex}} \sim 2\pi\frac{n_0\hbar^2}{m}\ln R\frac{\sqrt{mq}}{\hbar}. \tag{67}$$

We have dropped the contribution from the quadratic Zeeman term since it is independent of q.

This formula can be compared to the energy one expects for a *simple* vortex with the same charge $(2\pi,0)_3$,

$$E_{\text{vortex}} = I_E[(2\pi,0)_3]\pi\frac{n_0\hbar^2}{m}\ln\frac{R}{a_c'} + \epsilon_c, \tag{68}$$

which includes a core energy ϵ_c and introduces a parameter a_c' to allow us to redefine the core size physically. If we take $a_c'=L_q$, then the core energy has to be

$$\epsilon_c \approx \pi\frac{n_0\hbar^2}{m}\ln\frac{n_0\beta}{q}. \tag{69}$$

The core's energy is large when $q\to 0$ because it contains the point vortices.

C. Binding criteria

This example can be generalized using a set of binding criteria that ensure that a set of tetrahedral vortices will form a stable or metastable composite vortex. These criteria prevent a vortex molecule from breaking up into other molecules as illustrated in Fig. 7, even though the breakup may not violate charge or energy conservation.

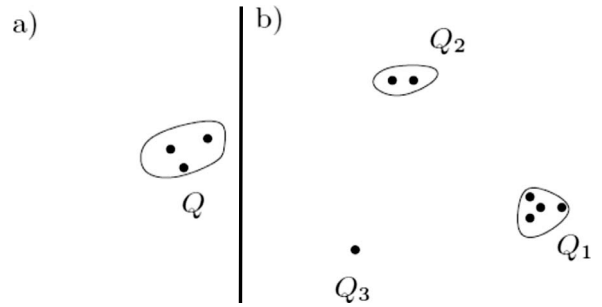

FIG. 7. Breakup of a molecule (a) which satisfies the binding criteria, but whose charge is not absolutely stable, into other composite vortices (b). If $Q=Q_3Q_2Q_1$ and $I_E(Q)>I_E(Q_1)+I_E(Q_2)+I_E(Q_3)$ then this process conserves charge and releases energy, but the breakup may still not occur spontaneously. If the component vortices in (b) are different from the component vortices in (a), then the vortices making up Q_1, Q_2, and Q_3 would have to be produced in a "chemical" reaction from the components of Q.

(1) Each component vortex is one of the stable $q=0$ vortices from Sec. V A and the net charge is aligned [see Eq. (36)].

(2) The kinetic energy would increase if any subset of the component vortices coalesced into a single vortex.

(3) There is no way for the component vortices to form submolecules that can break apart. This would occur if the components could be rearranged and then partitioned into r sets $\{\Gamma_1,\Gamma_2,\ldots,\Gamma_{j_1}\},\{\Gamma_{j_1+1},\Gamma_{j_1+2},\ldots,\Gamma j_1+j_2\},\ldots,\{\Gamma_{j_1+j_2+\cdots+j_{r-1}+1},\Gamma_{j_1+j_2+\cdots+j_{r-1}+2},\ldots,\Gamma_{j_1+j_2+\cdots+j_r}\}$ such that each subset forms a molecule *that is compatible with the magnetic field* [i.e., $\Pi_{i=j_1+\cdots+j_{k-1}+1}^{j_1+\cdots+j_k}\Gamma_i=(R_k^{m_k},2\pi[\frac{m_k}{3}+n_k])$] and such that the sum of the energy indices of these submolecules is less than the energy index of the original molecule.

The vortex molecule $(A,0)*(A,0)$ clearly satisfies all these conditions. Condition 1 is satisfied because $(A,0)$ is one of the stable vortices found in Sec. V A. Condition 2 is satisfied because the vortices repel each other. [For more vortices, since the Coulomb interaction Eq. (54) is not a sum of pairwise interactions, it is not enough to check that every *pair* of vortices repels each other.] Condition 3 is easy to check for a diatomic molecule such as this one, since it can only break up into individual "atoms;" neither of the fragments $(A,0)$ is compatible with the magnetic field.

D. Metastable vortices and how they decay

Not all of the vortex molecules satisfying the three conditions above are *absolutely* stable. The only absolutely stable *aligned* vortex types are

$$\pm\left(\frac{2\pi}{3},\frac{2\pi}{3}\right)_3, \quad \pm\left(\frac{2\pi}{3},-\frac{4\pi}{3}\right)_3. \tag{70}$$

For any *other* vortex topology $Q=(\alpha,\theta)_3$, one can find vortex topologies Q_i such that $\Pi_i Q_i=Q$ and

$$I_E(Q)>\sum_i I_E(Q_i). \tag{71}$$

Point vortices with such a topology Q would likely break apart spontaneously. (There is actually another pair of charges that could be absolutely stable, but the energy index estimate is not accurate enough to decide the issue

$$(0,\pm 2\pi)_3, \quad \left(\pm\frac{4\pi}{3},\mp\frac{2\pi}{3}\right)_3. \tag{72}$$

These vortices can break up into pairs without changing the net energy indices, reprising the ambiguous behavior of the two vortices at the end of Sec. V A. Section VI B decides the behavior of molecules with the second of these charges.)

There are some *composite* vortices of other charges besides the four listed in Eq. (70) which are long lived. The absolute stability criterion misses this possibility because it ignores the details of the vortex cores, drawing all its conclusions from the topology of the vortices far away; on the other hand the molecular binding criteria from Sec. VI C take the *contents* of the composite cores into account. Suppose the initial vortex Q is a cluster of vortices as illustrated in Fig. 7(a). The decay products discussed in the previous paragraph, Q_i, describe the topology of the final vortex clusters. The energy of the vortices after the reaction [Fig. 7(b)] is smaller if

$$E_{init}=I_E(Q)\pi\frac{n_0\hbar^2}{m}\ln\frac{R}{L}+k\ln\frac{L}{a_c}$$
$$>\sum_i\left[I_E(Q_i)\pi\frac{n_0\hbar^2}{m}\ln\frac{R}{L}+k_i\ln\frac{L}{a_c}\right]=E_{fin}. \tag{73}$$

The terms proportional to $\ln\frac{R}{L}$ stand for the kinetic energies outside the composite cores and the terms proportional to $\ln\frac{L}{a_c}$ stand for the energies within the composite cores; the latter contributions do not matter once the composite vortices are far apart ($R\gg L$). Therefore, the energy-index relation, Eq. (71), implies that the energy decreases when $Q\rightarrow Q_1*Q_2*\cdots Q_r$.

At zero temperature, a vortex molecule satisfying the binding criteria cannot break up even if the total energy would end up smaller. Although the metamorphosis of Fig. 7(a) into Fig. 7(b) lowers the energy, condition 3 states that the vortices in Fig. 7(b) are different than those in Fig. 7(a). Moreover, according to conditions 1 and 2, there are no spontaneous chemical reactions that can occur to make the components in Fig. 7(b) out of those in Fig. 7(a). Thus, at zero temperature, composite vortices besides the ones with charges listed in Eq. (70), whose energy indices seem to be too big, can still be stable.

The vortex molecule made up of $(A,0)*(A,0)$ is an example of a metastable vortex; it is not one of the absolutely stable charges $(2\pi,0)_3$ in Eq. (70) because its charge is the same as the net charge of the three *field-aligned* point vortices $(\frac{2\pi}{3},\frac{2\pi}{3})_3*(\frac{2\pi}{3},-\frac{4\pi}{3})_3*(\frac{2\pi}{3},\frac{2\pi}{3})_3$. The energy index of the molecule is $2(1^2)+0^2$ [see Eq. (52)] while the energy index of the three point vortices is smaller, $\frac{1}{3}+\frac{2}{3}+\frac{1}{3}$. Nevertheless, since these three vortices are not present in the core of the original vortex the decay cannot occur spontaneously.

At nonzero temperature, a molecule such as this, which satisfies the binding criteria but does not have a stable

charge, will only be metastable because a sequence of fusions and fragmentations can *in principle* transform Fig. 7(a) into Fig. 7(b). Some subsets of the original component vortices can fuse and the fused vortices can each break up into some other vortices. These would regroup into clusters each of which has a charge compatible with the magnetic field. Then each cluster would go its own way. (The fusion and fragmentation steps might sometimes happen more than once.) Conditions 1 and 2 ensure that at least one of the intermediate steps would be opposed by the Coulomb potential, but the *final* energy would decrease since the energy index decreases. The vortex molecule will be long lived because its components do not know that the hard effort of fusing will allow them to change into vortices which can separate.

Trial and error yields a couple of ways in which the $(A,0)*(A,0)$ bound state can break up. One possibility begins with the two-component vortices coalescing,

$$(A,0)*(A,0)\rightarrow(-id,0)\rightarrow\left(R,\frac{2\pi}{3}\right)*\left(R,\frac{2\pi}{3}\right)*\left(R,-\frac{4\pi}{3}\right). \tag{74}$$

The other begins when one of the components breaks up

$$(A,0)*(A,0)\rightarrow\left[\left(R^{-1},-\frac{2\pi}{3}\right)*\left(Q,\frac{2\pi}{3}\right)\right]*(A,0)\rightarrow\left(R^{-1},-\frac{2\pi}{3}\right)*\left[\left(Q,\frac{2\pi}{3}\right)*(A,0)\right]. \tag{75}$$

In the first process, the two vortices come together, increasing the kinetic energy in accordance with condition 2 [as shown by calculating the I_E's and substituting into Eq. (54)]. The resulting vortex breaks up into three vortices which can separate from each other because they are compatible with the magnetic field. The increase in energy during the first stage is given by $E_{s1}-E_{init}=\pi\frac{n_0\hbar^2}{m}\ln\frac{L_q}{a_c}$, where $E_{s1}=\pi\frac{n_0\hbar^2}{m}I_E\times(-id,0)\ln\frac{R}{a_c}$ is the energy of the intermediate vortex. Thermal fluctuations have a chance of driving the $(A,0)$'s together, in spite of the energy increase $E_{s1}-E_{init}$.

In the second process, Eq. (75), the $(A,0)$ vortex first splits up into two vortices. The first of these, $(R^{-1},-\frac{2\pi}{3})$, is compatible with the Zeeman field and can leave. The remaining two vortices stay bound because Q is a rotation around the wrong order 3 axis. In *this* process the energy increases during the initial fragmentation, according to condition 1. To check this, note that the energy of the intermediate state is

$$E_{s2}=\pi\frac{n_0\hbar^2}{m}\left\{\left[I_E\left(R^{-1},-\frac{2\pi}{3}\right)+I_E\left(Q,\frac{2\pi}{3}\right)+I_E(A,0)\right]\ln\frac{L}{a_c}+I_E(-id,0)\ln\frac{R}{L}\right\} \tag{76}$$

and the energy barrier is

$$E_{s2}-E_{init}=\pi\frac{n_0\hbar^2}{m}\left[I_E\left(R^{-1},-\frac{2\pi}{3}\right)+I_E\left(Q,\frac{2\pi}{3}\right)-I_E(A,0)\right]\ln\frac{L}{a_c}=\frac{\pi n_0\hbar^2 m}{6}\ln\frac{L}{a_c}. \tag{77}$$

This energy barrier is lower than $E_{s1}-E_{init}$, so Eq. (75) is a more common breakup route. (In a finite condensate, thermally excited breakups can be observed only if a vortex molecule is somehow prevented from wandering to the boundary of the condensate and annihilating before it can decay.)

These two examples illustrate the meaning of the binding conditions. Conditions 1 and 2 ensure that fragmentation and fusion processes cannot happen spontaneously. The third condition simply points out that vortex clusters such as $(A,0)^2*(B,0)^2$ will not be stable because the components can sort themselves into field-aligned groups and break up without any thermal assistance.

The second condition can be difficult to check for a composite vortex with three or more subvortices. One must consider subsets of every size and check that they cannot lower their energy by collapsing all at once into one vortex. An example is the set of three vortices $(A,0)^3$ discussed at the end of Sec. IV B. An even more counterintuitive complication is that, because of the noncommutative behavior of the combination rules, more complicated fusion processes can occur. A vortex can change its type by circling around one vortex so that it can fuse with another vortex (see Appendix B). For a bound state of many vortices there will be many possibilities for how the components meander around each other before some of them fuse. To test condition 3, one also has to enumerate all possible wanderings.

A mathematical consequence of this discussion is that there is a solution to the time-independent Gross-Pitaevskii equation for each set of vortex topologies that satisfy the binding conditions. An approximate wave function such as Eq. (61) will relax to an exact solution without any change in its topology. The topology cannot change because the energy of the initial configuration is less than the energy of the states at the tops of the barriers it needs to cross. (Though we have not calculated the energy of these intermediate states precisely, any errors are small compared to the logarithmic barrier height.)

VI. ADDITIONAL EXAMPLES

Now we can construct some other, more interesting, examples (see Table I). We will use the algebra of the group of vortex charges to find molecules whose net charge is interesting in different ways and we will use the energy index to test whether they are stable.

The parameter c will be less than 4 for some of these examples, so that an order-2 axis of the tetrahedron will line up with the z axis when it is in its ground state. The aligned topologies have the forms $(\pi n,2\pi m)_2$, as described in Sec. III B. Of these, the only absolutely stable topologies are $\pm(\pi,0)_2$ and $\pm(0,2\pi)_2$ [and $(\pm\pi,\pm2\pi)_2$ are ambiguous cases].

A. Doubly-quantized pure phase vortex

First let us find a vortex molecule whose phase winds by 4π. In single-component condensates, such vortices are usually unstable; one has been observed to break up, maybe into an entwined pair of 2π vortices.[36] If phase and spin textures were completely independent of one another, doubly-quantized vortices would not be any more stable in the cyclic condensates, but fractional circulations are "bound" to certain spin textures (see Sec. III B). *If* we assume the vortex $(R,-\frac{4\pi}{3})$ is stable (at the end of Sec. V A we could not decide), then a doubly-quantized vortex can occur in a cyclic condensate when $c<4$. It consists of the three parts

$$\left(P^{-1},\frac{4\pi}{3}\right)\left(Q^{-1},\frac{4\pi}{3}\right)\left(R^{-1},\frac{4\pi}{3}\right). \tag{78}$$

The phase changes by 4π while the orientation of the tetrahedron does not change at infinity as we can check using the coordinate system from Fig. 2(b). The three group elements are

$$P^{-1}=\frac{1}{2}[1+i(\sigma_x-\sigma_y-\sigma_z)],$$

$$Q^{-1}=\frac{1}{2}[1+i(\sigma_x+\sigma_y+\sigma_z)],$$

$$R^{-1}=\frac{1}{2}[1+i(\sigma_z-\sigma_x-\sigma_y)],$$

and their product is the identity.

Let us now check as many of the conditions for binding as we can so far. Condition 1 is not easy to check because $(P^{-1},\frac{4\pi}{3})$ has the same charge and energy index as $(R,\frac{2\pi}{3})*(Q,\frac{2\pi}{3})$, so the single vortex and the pair have energies differing by a finite amount. An accurate solution for the spin texture around the pair is needed to determine the sign of the energy difference. In fact the stability of $(P^{-1},\frac{4\pi}{3})$ might depend on the value of c. Let us therefore hope that condition 1 is satisfied. Condition 3 is clear since the aligned vortices are order-2 vortices when $c<4$. To check condition 2, let us first consider whether one of the *pairs* of vortices in the trio can coalesce. Using conservation of topological charge helps to avoid enumerating all the ways the vortices can braid around each other. If the first two vortices have coalesced into a vortex $(X,\frac{8\pi}{3})$ (after some permutation) and the third vortex, by winding around the other two vortices as they collapsed, has changed to $(Y^{-1},\frac{4\pi}{3})$, then

$$(XY^{-1},4\pi)=(id,4\pi) \tag{79}$$

by conservation of charge. Hence $X=Y$. Also, braiding one vortex between other vortices can only *conjugate* its group element. Therefore, Y, like R, is a counterclockwise rotation through 120°. Since $X=Y$, the rotation part of the coalesced vortex $(X,\frac{8\pi}{3})$ also is a 120° turn and thus the energy index of this coalesced vortex is $2\times(1/3)^2+(4/3)^2=2$, which is *greater* than the sum of the energy indices of the two vortices which formed it. Therefore the two vortices cannot coalesce spontaneously. (This argument can be generalized to any trio of vortices $\Gamma_1,\Gamma_2,\Gamma_3$ each of which commutes with the net charge Γ. Fusing two of the vortices gives the same result (up to conjugacy) no matter how the vortices are mixed around first, so braiding cannot make a repulsive interaction between two vortices into an attractive one.) The justification of condition 2 is completed by noting that the three vortices cannot coalesce simultaneously because $I_E(0,4\pi)>I_E(P^{-1},\frac{4\pi}{3})+I_E(Q^{-1},\frac{4\pi}{3})+I_E(R^{-1},\frac{4\pi}{3})$.

B. Vortex molecule which is stable

We now return to the assumption $c>4$ and show that there is an *absolutely* stable vortex with charge $(-\frac{4\pi}{3},\frac{2\pi}{3})_3$, answering the question raised at the beginning of Sec. V D. The two point vortices

$$\left(-\frac{2\pi}{3},-\frac{2\pi}{3}\right)_3*\left(-\frac{2\pi}{3},\frac{4\pi}{3}\right)_3 \tag{80}$$

have the same energy index and topology as a vortex of charge $(-\frac{4\pi}{3},\frac{2\pi}{3})_3$. Therefore, it is unclear whether a point vortex of this latter charge could lower its energy by breaking up. But there is a vortex *molecule* with the same charge whose energy is lower by a large (but still finite) amount than the energy $\frac{\pi n_0\hbar^2}{m}(\frac{1}{3}+\frac{2}{3})\ln\frac{R}{a_c}$ of the pair. This molecule is formed of the two lowest energy fragments that $(\frac{-4\pi}{3},\frac{2\pi}{3})_3\equiv(R^{-2},\frac{2\pi}{3})$ could break up into in the *absence* of a magnetic field

$$\left(-\frac{4\pi}{3},\frac{2\pi}{3}\right)_3\equiv\left(R^{-2},\frac{2\pi}{3}\right)\rightarrow\left(Q,\frac{2\pi}{3}\right)*(A,0). \tag{81}$$

In a magnetic field, the two vortices will still move apart a distance of about L_q, decreasing the energy by

$$\Delta E=\left[I_E\left(R^{-2},\frac{2\pi}{3}\right)-I_E\left(Q,\frac{2\pi}{3}\right)-I_E(A,0)\right]\frac{\pi n_0\hbar^2}{m}\ln\frac{L_q}{a_c}$$
$$=\frac{1}{6}\frac{n_0\pi\hbar^2}{m}\ln\frac{L_q}{a_c}. \tag{82}$$

The resultant molecule has a lower energy than the pair of unbound vortices in Eq. (80), since the breakup in Eq. (80) lowers the energy by only an amount on the order of the magnetic core energies (if it does lower the energy). The molecule is therefore absolutely stable.

To take another point of view, in a computer simulation, one might impose the topology $(-\frac{4\pi}{3},\frac{2\pi}{3})_3$ far away and minimize the energy. The wave function obtained then has an asymmetric structure: it has two "singularities" with topologies $(Q,\frac{2\pi}{3})$ and $(A,0)$ at a distance of order L_q. By contrast, when the topology imposed at a boundary corresponds to an unstable vortex, the ground state has singularities whose spacing is on the order of the size of the system R, e.g., for a scalar condensate one might try to impose $\psi(R,\phi)=\sqrt{n_0}e^{2i\phi}$. The spacing of the vortices in the energy minimizing wave function grows with R, reflecting the fact that these vortices would repel each other to infinity in an infinite condensate.

C. "Bound state" of no vortices

The final example shows that tetrahedral point vortices are not necessary to hold a composite core together—there is a "composite" vortex which does not contain any tetrahedral cores for both $c<4$ and $c>4$.

The necessity of using SU_2 instead of SO_3 is the biggest surprise to come out of the theory of vortex charge. While an $\alpha=2\pi$ vortex cannot relax, an $\alpha=4\pi$ "vortex" can relax continuously to a uniform state in the absence of a magnetic field. This relaxation process is described by

$$\psi(\phi;t)=e^{-i\phi(F_x \sin \pi t+F_z \cos \pi t)}e^{-iF_z\phi}\sqrt{n_0}\chi_0, \tag{83}$$

as the time t runs from 0 to 1. (χ_0 is an arbitrary cyclic spinor.)

On the other hand the group $G_q=\{(\alpha,\theta)\}$ used to describe aligned charges distinguishes even charges for which α differs by multiples of 4π: the rotational symmetries of the Hamiltonian form a circle, which has to be completely unwound into a line in order to give different names to all pairs of topologically distinct charges. Therefore the aligned charges are not a subset of the tetrahedral charges. Instead, there is a many-to-one mapping from aligned to tetrahedral charges $Q\in G_q\rightarrow r(Q)\in G$ describing what the aligned charge Q evolves into when the anisotropy is turned off. (See Ref. 60 for a discussion of the relationships between topological charges as symmetry is reduced.)

The tetrahedral charges Γ_i of the components of a molecule determine only $r(Q)$, as Eq. (36) implies. In general

$$r(Q)=\prod_i \Gamma_i. \tag{84}$$

For a given set of component charges, Eq. (36) determines only $m(\mathrm{mod}\ 6)$ and $(\frac{m}{3}+n)$. In particular, a vortex with no tetrahedral vortices in it may have $Q=(4\pi,0)_{2,3}$.

In fact, suppose $c>4$ and imagine bringing four $(\frac{2\pi}{3},\frac{2\pi}{3})_3$ and two $(\frac{2\pi}{3},-\frac{4\pi}{3})_3$ vortices together. When these four vortices are close enough together, they behave as tetrahedral vortices and they annihilate since $R^6=id$. The vortex field at infinity cannot relax via Eq. (83) because $\alpha=4\pi$ is conserved at nonzero q, so a coreless vortex must remain.

Equation (83) can be reused to describe this vortex's qualitative form. We replace the time coordinate by a function of the radius to give a singularity-free spin texture that winds through 4π at infinity

$$\psi=\psi\left(\phi;\frac{1}{1+\left(\frac{r}{L_q}\right)^2}\right). \tag{85}$$

This vortex is not *absolutely* stable since two $(2\pi,0)_{2,3}$'s have a smaller energy, but it is obviously metastable—there are no vortices in the core to break apart. The vortex can only break up if thermal energy causes a vortex-antivortex pair to nucleate in the core. A pair of $\alpha=\pm 2\pi$ vortices initially attracts each other but if the thermal fluctuations pull them to opposite sides of the core the nonlinear coupling with the background field switches this force from attractive to repulsive and the vortex decays.

VII. CREATING AND OBSERVING VORTEX MOLECULES

If an atom whose ground state is cyclic can be found (or simulated), one can study the cyclic phase in an experiment even without perfectly canceling the earth's magnetic field by studying vortex-molecule cores. Let us discuss the conditions under which these Zeeman-effect bound states might be observed and the methods one can use for observing them. First of all, we must assume that $q\ll\beta n_0$ in order to justify neglecting q near the tetrahedral vortices and to justify the perturbation theory of Sec. IV A. This is not just a technical assumption: above a certain magnetic field the component vortices probably merge. To estimate the maximum magnetic field note that q is related to the hyperfine splitting A_{HF} via

$$|q|=\frac{\mu_B^2B^2}{8A_{HF}}, \tag{86}$$

for rubidium and sodium atoms,[3] and similar relations hold for other atoms. Also note that the spin-independent interaction is

$$\alpha=\frac{4\pi\hbar^2}{ma}, \tag{87}$$

where $a\sim 50$ Å is an *average* of the scattering lengths corresponding to different net spins and that the spin-dependent interaction is

$$\beta=\frac{4\pi\hbar^2\Delta a}{m}, \tag{88}$$

where $\Delta a\sim 1$ Å (Refs. 44 and 46) depends on the *differences* between the scattering lengths.[11] The condition for our analysis to be applicable, $q\ll n_0\beta$, therefore implies

$$B\ll B_{Max}\sim\frac{1}{\mu_B}\sqrt{A_{HF}\frac{\hbar^2n_0\Delta a}{m}}, \tag{89}$$

about 0.1 G for a condensate of rubidium atoms with density $n_0=5\times 10^{14}/\mathrm{cc}$.

In order to observe vortex-bound states, one might start with a condensate prepared with a spin order other than the ground state and then watch it evolve as in Ref. 8. Thermal (and less importantly, quantum) noise will produce perturbations that grow exponentially, producing complicated patterns. If the magnetic field is small enough, vortex-bound states might be found after some time. One could also take a more deliberate approach, choosing tetrahedral vortex types and imprinting them as in Ref. 34 or 61. One can then observe the vortices' dynamics.

In fact, identifying the vortices that appear in a spinor condensate is difficult because they have nearly the same density as the rest of the condensate.[62] One thus has to measure something about the spins to observe the vortices. Two possibilities have already been invented. One can either measure the magnetization field as in Ref. 8 or use Stern-Gerlach separation to measure the density of the different spin species.

One cannot observe the magnetization direction varying around a vortex in the cyclic phase as one can in the ferromagnetic phase studied in Ref. 8. There is no magnetization

[see Eq. (50)] except inside the core, where the order parameter leaves the ground-state space $\mathcal{M}$. But measuring the magnetic moment in the core of a vortex helps to determine the topological charge of the vortex. Any vortex one might have to identify involves a rotation about an arbitrary axis $\hat{\boldsymbol{n}}'$ as in Eq. (25) or the more convenient Eq. (26). The latter description starts with a vortex whose rotation axis is special—say it is parallel to $\hat{z}$—and applies some overall rotations to it.

For example, a vortex of type $(R, \frac{2\pi}{3})$ is described according to Eq. (26) by

$$\psi(r,\phi) = D(R)e^{i/3(1+F_z)\phi}\sqrt{n_0}\left(f(r)\sqrt{\frac{1}{3}},0,0,g(r)\sqrt{\frac{2}{3}},0\right)^T$$
$$= D(R)\sqrt{n_0}\left(f(r)e^{i\phi}\sqrt{\frac{1}{3}},0,0,g(r)\sqrt{\frac{2}{3}},0\right)^T, \quad (90)$$

where $f(r)$ and $g(r)$ are appropriate functions approaching 1 at infinity and R is a rotation that moves $\hat{\boldsymbol{n}}=-\hat{z}$ to $\hat{\boldsymbol{n}}'$. If $\hat{\boldsymbol{n}}'=\hat{\boldsymbol{n}}=-\hat{z}$, then R is the identity, so $m_x(r)=m_y(r)=0$ and

$$m_z(r,\phi) = \psi(r,\phi)^\dagger F_z \psi(r,\phi) = \frac{2}{3}[f(r)^2 - g(r)^2]n_0. \quad (91)$$

Hence, the magnetization is parallel to the symmetry axis and is given by $\boldsymbol{m}=\frac{2}{3}n_0[g(r)^2-f(r)^2]\hat{\boldsymbol{n}}$. Applying an arbitrary reorientation R changes the magnetization axis and the symmetry axis in the same way, so the general result is

$$\boldsymbol{m} = \frac{2}{3}n_0[g(r)^2 - f(r)^2]\hat{\boldsymbol{n}}'. \quad (92)$$

The magnetization inside the core can be found by noting that the top component of the vortex Eq. (90) must vanish at $r=0$ in order to be continuous,

$$f(0) = 0. \quad (93)$$

Since α is much larger than β and γ, the density of atoms will be almost uniform across the whole vortex and hence $\frac{1}{3}f(r)^2+\frac{2}{3}g(r)^2\approx 1$. Equation (93) therefore implies

$$g(0) \approx \sqrt{\frac{3}{2}}. \quad (94)$$

Hence the core magnetization, Eq. (92), is approximately $n_0\hat{\boldsymbol{n}}'$; the atoms have a single unit of hyperfine spin in the direction of the vector from the center to the *fixed* vertex of the rotating tetrahedra near vortex the core.[63] The inverse vortex, $(R^{-1}, -\frac{2\pi}{3})$, has the same core magnetization (it does not change sign). On the other hand, similar arguments show that $(R, -\frac{4\pi}{3})$ will have a magnetization approximately equal to $-2n_0\hat{\boldsymbol{n}}'$ at the core center because, in this case, the $m=-1$ component of the spinor has the phase winding before $D(R)$ is applied. The third stable vortex type, $(A,0)$, will not have any magnetization in its center. Thus, measuring the magnetization reveals vortices of order 3 but does not distinguish between vortices and antivortices and does not even indicate the presence of an order 2 vortex. (Measuring the magnetization gives enough information to observe the vortex molecule in Sec. VI A.) Another difficulty is that the cores are small: only about 1 μm across. However, one could first allow the condensate to expand in the transverse direction so that the atomic interactions decrease. The vortex cores would expand; as in experimental observations of vortices in single-component condensates, the depleted region in f or g (whichever corresponds to the component of the transformed spinor with the phase winding) would fly apart. A magnetized ring would form at the edge of the core where the atoms of one magnetization accumulate more than the atoms of the other.

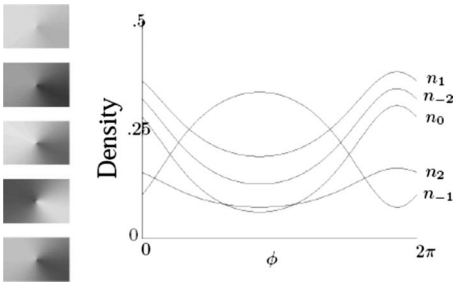

FIG. 8. Densities in the five spinor components around an order-3 vortex, with a randomly oriented local axis $\hat{\boldsymbol{n}}'$. On the left is the pattern one might observe experimentally; the lighter regions correspond to regions with fewer atoms. On the right are plotted the percentage of atoms for each value of F_z at some fixed distance from the vortex core. The phases and amplitudes of these oscillations should help to determine the direction of the local axis.

The Stern-Gerlach method gives more information about the vortices. Spin vortices produce observable patterns in the condensates' Stern-Gerlach images. These images capture separately the density of atoms in each of the five components of the spinor as functions of position. In these density profiles each vortex (aside from pure phase vortices) will be ornamented by radiating density ripples as illustrated in Fig. 8. While a vortex in a condensate of a single type of atom does not show any density modulation (unless the condensate interferes with a second condensate, see, e.g., Ref. 64), interference between the f and g components of the spinor occurs as a result of the unitary transformation changing the quantization axis from the vortex's rotation axis $\hat{\boldsymbol{n}}'$ to the magnetic field direction. For the vortex described by Eq. (90), the density of atoms with $F_z=m$ is given by

$$\frac{n(r,\phi,m)}{n_0} = \left| D_{m2}(R)\sqrt{\frac{1}{3}}f(r)e^{i\phi} + D_{m,-1}(R)\sqrt{\frac{2}{3}}g(r)\right|^2$$
$$= a_m + b_m\cos(\phi-\phi_m), \quad (95)$$

where a_m, b_m are constants outside the vortex cores, since $f(r)$ and $g(r)$ approach 1. If the $\hat{\boldsymbol{n}}'$ axis happens to line up exactly with the axis of the Stern-Gerlach field, then there are no radial "interference fringes." However, the tetrahedral vortices in a composite vortex tend to interact so as to favor tilted axes $\hat{\boldsymbol{n}}'$, as illustrated by the qualitative wave function in Sec. V [see Eq. (65)].

Both the order 3 and order 2 vortices will be identifiable with the help of the Stern-Gerlach images. One can deduce the types of the vortices and their axes $\hat{\boldsymbol{n}}'$ [which are en-

coded in $D(R)$] by measuring the average magnitudes, a_m, of the densities together with the amplitudes b_m and offsets ϕ_m of the density *modulations*. [An order 2 vortex will have $\cos 2\phi$ and $\sin 2\phi$ Fourier modes in addition to the terms given in Eq. (95).] A possible difficulty with this method arises because, once the five spin components are separated in space, the density oscillations in each of them are no longer stable. The ensuing dynamics in the clouds could mix the atoms up. Distinguishing among vortices with the same rotation but different phase winding numbers, such as $(R, \frac{2\pi}{3})$ and $(R, -\frac{4\pi}{3})$, is not possible with this method without resolving the cores.

One would also hope to check some predictions about the size and charges of the bound states. One can select clusters of vortices in an image of the condensate (if there are not too many vortices) and use the methods just discussed to identify the vortex charges and check that each cluster satisfies Eq. (36). Additionally, a sign that the vortex clusters are actually *bound* states is that the bound state size depends in the right way on the magnetic field. For the cyclic phase, Eq. (10) can be expressed in terms of the scattering lengths as

$$L_q \sim \sqrt{n_0 \Delta a} \frac{\hbar^2}{mq} \quad \text{for cyclic phase.} \tag{96}$$

Atoms whose ground state is cyclic may be difficult to find (^{87}Rb is likely to be polar,[44] though it may be possible to adjust the interaction parameters by applying light fields). The general method of this paper can also be applied to spin-3 condensates (see Ref. 65), as well as to spin-1 condensates and pseudospin-$\frac{1}{2}$ condensates as already studied by Refs. 17 and 18. For these phases the orientation dependence of the energy is a direct consequence of the Zeeman effect (unlike in the cyclic phase, see Sec. IV A), so $V_{eff} \sim q n_0$. Hence

$$L_q \sim \frac{\hbar}{\sqrt{mq}} \quad \text{for phases with} \quad V_{eff} \propto q. \tag{97}$$

Since $q = \frac{\mu_B^2 B^2}{8 A_{HF}}$, the size of the molecules in the cyclic phase is proportional to $\frac{1}{B^2}$ and the size of molecules in phases with $V_{eff} \propto q$ is proportional to $\frac{1}{B}$.

The size of the condensate must be several times larger than a vortex molecule at B_{Max} in order to see the size variation. The smallest vortex molecule occurs at around B_{Max} [see Eq. (89)] and has a size of $L_q(B_{Max}) \sim \frac{1}{\sqrt{\Delta a n_0}} \sim a_c$, which is the same as the typical size of the component cores, a_c. This is of order 1 μm.

Because the size of the molecule at B_{Max} is the same as the size of the vortices making it up, vortex molecules probably undergo transitions at fields close to B_{Max} (see Fig. 9). Absolutely stable vortex molecules, such as example 3 in Table I, will be compressed so that the cores coincide and the vortex might become rotationally symmetric at a finite field. Once the components' cores overlap a little bit, being slightly offset might not lead to significant savings in kinetic energy. On the other hand, when the vortices in a *metastable* molecule are squeezed together, they form an unstable tetrahedral vortex so they cannot survive anymore.

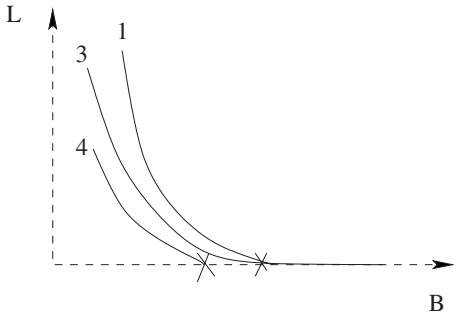

FIG. 9. The evolution of vortex molecules as the magnetic field is increased. The three curves illustrate how the sizes of the molecules from Table I, for $c>4$, might change as the strength of the magnetic field is increased. The sizes decrease as $\frac{1}{B^2}$. At a certain magnetic field, an absolutely stable vortex might become rotationally symmetric (molecule 3). Metastable vortices will become unstable when a certain magnetic field is reached, indicated by the x's terminating the curves corresponding to molecules 1 and 4.

VIII. CONCLUSION

We have illustrated how a hierarchy in an order-parameter space can cause vortices to form molecules. Hierarchy can be created in the cyclic phase by applying a weak magnetic field. Such a field produces an anisotropic potential for the tetrahedron describing the cyclic phase and leads to a transition between phases with order-2 and order-3 symmetries (see Fig. 2), which consequently have different types of vortex molecules.

Vortex molecules can be understood using just qualitative group theory and energy estimates. They illustrate visually the relationship between the symmetries with and without the magnetic field, as the binding criteria [see Eq. (36) and Sec. V C] emphasize. The component vortices correspond to symmetries of the more symmetric phase at $B=0$. The external field of the vortex will behave as one expects for a nonzero magnetic field. The core grows in size as $\frac{1}{B^2}$ as the magnetic field is decreased.

Most surprisingly, high-energy defects can be long lived. In a system that can have topological defects, the defects with higher charges can break up into smaller charges while lowering their energy and the most conservative assumption is that the higher-charge defects will not be seen (unless they are pinned by a wire, for example). However, in weak magnetic fields, the cores are simple enough that we can be sure that some of the defects with big charges will be long lived. Doubly-quantized spin-current vortices (and maybe also charge-current vortices) are metastable, for example (see Sec. VI). Table I lists all the vortex molecules discussed.

The component vortices are subject to the *approximate* generalization of Coulomb's law [see Eq. (54)]. When these forces are repulsive, the vortex molecule is stable at zero temperature. But a molecule can break up when thermal fluctuations overcome these repulsions. The possible breakup "channels" for a metastable vortex are reminiscent of decay processes in nuclear physics. [In practice, the molecules probably will not survive long enough for "ultracold fusion" (or fission) to happen.] The breakup channels can be found by trial and error, keeping in mind the topological conserva-

tion laws, as illustrated in Sec. V D. Molecule 1 is most likely to break up into a vortex atom and a stable vortex molecule [see Eq. (75)].

We can predict a variety of phenomena involving vortex-bound states, even though we have not made detailed calculations, because the cyclic phase has so many symmetries. More accurate calculations of the vortex fields and energies would address other interesting questions, such as the following two. First, we would like to understand tetrahedral vortices without magnetic fields better. For example, the rough estimates are not always sufficient to determine whether a vortex is absolutely stable or not. The stability of vortex 2 in the table hinges on this issue. The component $(R,-\frac{4\pi}{3})$ can break up into a pair of vortices which do not have a long-range interaction (see Sec. V A): the energy index estimate shows that the energy changes by a finite amount when the fragments are separated, but whether the change is *positive* or *negative* is not clear. Also, the "conservative hypothesis" that tetrahedral vortices are either absolutely stable or else will decay spontaneously may not be correct. Second, can a molecule at a nonzero magnetic field have multiple stable spatial arrangements of its components? A more accurate understanding of the kinetic-energy landscape would be a starting point for answering this question.

ACKNOWLEDGMENTS

We wish to thank R. L. Barnett, M. Greiner, H. Y. Kee, J. Moore, S. Mukerjee, K. Sengstock, D. Stamper-Kurn, and W. P. Wong for useful conversations. We also acknowledge financial support from CUA, DARPA, MURI, USAFOSR, and NSF under Grant No. 0705472.

APPENDIX A: FINDING THE EFFECTIVE ACTION

Equation (44) is not as difficult to minimize as it appears because of the special symmetry of χ_2. We must substitute $\tilde{\psi}=\sqrt{n_0}\chi_2+\delta\tilde{\psi}$, where

$$\delta\tilde{\psi}=d\chi_2+aF_x\chi_2+bF_y\chi_2+cF_z\chi_2+(e+if)\chi_{2t}, \quad \text{(A1)}$$

into the energy V_{tot} given by Eq. (44). The perturbation $\delta\tilde{\psi}$ is the deformation of the tetrahedron measured relative to its body axes. Let us figure out which powers of the coefficients $a,b,\ldots$ to keep at each stage of calculating V_{tot}. This is easiest if one starts by completing the square in Eq. (44) to get

$$V_{tot}(\psi)=\frac{1}{2}\alpha(\tilde{\psi}^\dagger\tilde{\psi}-n_0)^2+\frac{1}{2}\beta(\tilde{\psi}^\dagger\mathbf{F}\tilde{\psi})^2+\frac{1}{2}\gamma|\tilde{\psi}_t^\dagger\tilde{\psi}|^2-\frac{1}{2}\alpha n_0^2-q\sum_{i,j=1}^{3}\cos\alpha_i\cos\alpha_j\tilde{\psi}^\dagger F_iF_j\tilde{\psi}, \quad \text{(A2)}$$

where we note that the chemical potential for the cyclic state is $\mu=\alpha n_0$ and define $\gamma=c\beta$. We also use $F_{1,2,3}$ to stand for $F_{x,y,z}$. We need to find the minimum of this energy only to quadratic order in q. At the end we will find that $a,b,c,\ldots$ are each *linear* in q. Since each of the quantities squared in the first three terms of V_{tot} vanishes when $a,b,c,\ldots=0$, just the *linear* contributions from $a,b,c,\ldots$ give the potential to *quadratic* order in q. The quadratic Zeeman term, since it is multiplied by q, also is not needed beyond linear order in a,b,c,d,e, and f.

Next find which matrix elements of χ_2 need to be calculated to evaluate all these contributions to the energy. When calculating an expectation value of the form $\tilde{\psi}^\dagger M\tilde{\psi}=(\sqrt{n_0}\chi_2+\delta\tilde{\psi})^\dagger M(\sqrt{n_0}\chi_2+\delta\tilde{\psi})$, only the cross terms between the unperturbed part $\sqrt{n_0}\chi_2$ and the perturbation give linear functions of a,b,c,d,e, and f. For example, one cross term contained in the quadratic Zeeman contribution is

$$\tilde{\psi}^\dagger F_xF_y\tilde{\psi}\approx n_0\chi_2^\dagger F_xF_y\chi_2+2\sqrt{n_0}\Re\chi_2^\dagger F_xF_y[(aF_x+bF_y+cF_z+d)\chi_2+(e+if)\chi_{2t}]. \quad \text{(A3)}$$

Expanding this gives a sum of matrix elements such as $\chi_2^\dagger F_xF_y\chi_2$ and $\chi_{2t}^\dagger F_xF_yF_z\chi_2$. Therefore, we need only the matrix elements of products of at most three F's. Many of these (e.g., $\chi_2^\dagger F_iF_jF_k\chi_2$ when i,j,k are not all different and $\chi_{2t}^\dagger F_iF_j\chi_2$ when i and j are different) are equal to zero because of the 180° symmetries of χ_2 around the coordinate axes. The numerical values of the few remaining ones can be worked out quickly. Using these matrix elements to calculate all the terms in Eq. (A2) produces an expression $V_{tot}(a,b,c,d,e,f,\cos\alpha_1,\cos\alpha_2,\cos\alpha_3)$. Along the way, one notices that each of the variables $a,b,c,\ldots$ contributes to only one term of the energy in zero-magnetic field [the first line of Eq. (A2)]. That is, the variables a,b,c determine the magnetization, d determines the density perturbation, and e and f determine the singlet amplitude θ, e.g.,

$$n=n_0+2\sqrt{n_0}d,$$

$$M_x=4\sqrt{n_0}a,$$

$$\Re[\theta]=2\sqrt{n_0}e. \quad \text{(A4)}$$

Finally, minimize the potential. It can be written as a sum of independent quadratic functions of a,b,c,d,e, and f,

$$V_{tot}=\left(-\frac{1}{2}\alpha n_0^2+2qn_0\right)+2\alpha n_0d^2-4\sqrt{n_0}qd+8\beta n_0(a^2+b^2+c^2)+4\sqrt{3n_0}q(a\cos\alpha_2\cos\alpha_3+b\cos\alpha_1\cos\alpha_3+c\cos\alpha_1\cos\alpha_2)+2\gamma n_0(e^2+f^2)+2q\sqrt{n_0}[e(\cos^2\alpha_1+\cos^2\alpha_2-2\cos^2\alpha_3)+\sqrt{3}f(\cos^2\alpha_1-\cos^2\alpha_2)]. \quad \text{(A5)}$$

(Note that the second term, $2qn_0$, is the first-order contribution of the Zeeman energy, which is independent of orientation.)

Minimizing each quadratic (which gives $a=-\frac{\sqrt{3}q}{4\beta\sqrt{n_0}}\cos\alpha_2\cos\alpha_3,\ldots$) and combining the results together with the help of Eq. (42) give

$$V_{eff} = -\frac{1}{2}\alpha n_0^2 + 2qn_0 - 2\frac{q^2}{\alpha} + \frac{q^2}{\gamma} - \frac{3q^2}{4\beta} + \left(\frac{3q^2}{4\beta} - \frac{3q^2}{\gamma}\right) \times (\cos\alpha_1^4 + \cos\alpha_2^4 + \cos\alpha_3^4). \quad \text{(A6)}$$

All the constant terms can be dropped to give Eq. (5). Note that the magnetization varies with the orientation of the tetrahedron [as can be checked by substituting the optimal values for a,b,c into the magnetization, Eq. (A4)]. In particular, the $c>4$ ground state with $\cos\alpha_1,\cos\alpha_2,\cos\alpha_3 = \pm\frac{1}{\sqrt{3}}$ has a small magnetization, $\boldsymbol{m} = \mp\frac{q}{\beta\sqrt{3}}(1,1,1)$; since this has been calculated from $\tilde{\psi}$, it is the magnetization *relative to the body axes*. Comparing this to the magnetic field relative to the body axes, $B(\cos\alpha_1,\cos\alpha_2,\cos\alpha_3) = \frac{B}{\sqrt{3}}(1,1,1)$, shows that the magnetization is either parallel or antiparallel to the magnetic field.

The effective potential allows us to eliminate the six most rigid degrees of freedom corresponding to a,b,c,d,e, and f; the purpose is to make vortex textures easier to describe by concentrating on the rephasing and rotation angles as a function of position. The wave function in Eq. (16) can be parameterized in terms of Euler angles for the rotation, e.g., $\psi = \sqrt{n_0}e^{i\sigma F_z}e^{i\tau F_x}e^{i\rho F_z}e^{i\theta}\chi_2$. One can check that $\cos\alpha_1 = \sin\tau\sin\rho$, $\cos\alpha_2 = -\sin\tau\cos\rho$, and $\cos\alpha_3 = \cos\tau$. The first angle, σ, does not appear because the tetrahedron can be rotated around the z axis without changing the angles α_i. Now, working out the kinetic energy and combining it with the effective potential gives the "phase-and-rotation-only" energy functional

$$\mathcal{E}_{eff} = \int\int d^2\mathbf{r}\frac{n_0\hbar^2}{2m}[2(\nabla\rho)^2 + 2(\nabla\tau)^2 + 2(\nabla\sigma)^2 + (\nabla\theta)^2 + 4\cos\tau\nabla\sigma\nabla\rho] + (c-4)\frac{3q^2}{4c\beta}[\cos^4\tau + \sin^4\tau(\sin^4\rho + \cos^4\rho)]. \quad \text{(A7)}$$

This can be solved (in principle) to give the textures around sets of vortices and the relative positions of the vortices in equilibrium. Each vortex type implies a certain type of discontinuity in the four angles as the core is encircled. This expression does not seem too easy to use, but at least it shows just the two effects we have been balancing against one another (kinetic and anisotropy energies). The size of vortex molecules can be found more precisely than in the body of the paper by assuming that the two terms are comparable, $\frac{n_0\hbar^2}{mL_q^2} \sim |c-4|\frac{q^2}{c\beta}$. Hence, $L_q \propto \frac{1}{\sqrt{|c-4|}}$. Rescaling by L_q leads to an energy function depending only on the *sign* of $c-4$. Therefore, in a molecule with three vortices, the angles of the triangle they form will be independent of all the parameters, including c, even though it is dimensionless.

Equation (A7) is derived from Eq. (3) by determining how the tetrahedra are distorted by the quadratic Zeeman effect. But the kinetic energy also causes distortions of the wave function from the perfect tetrahedral form and it seems possible that these distortions could lead to kinetic effects in the anisotropy term and anisotropy effects in the kinetic-energy term. However, at the lowest order, treating the two terms independently seems correct. A simple argument for this (neglecting the kinetic energy when finding the anisotropy potential) is that the distortion due to the Zeeman term is linear in q while the distortion due to the kinetic energy is quadratic in q. To see this, think of an ordinary scalar vortex, where the density varies as $n_0(1-\frac{a_c^2}{r^2})$ far from the core.[3] The amount of "distortion" is $-\frac{a_c^2}{r^2}n_0$. In the cyclic state, distortion (i.e., perturbations to the spinor components that take it out of $\mathcal{M}$) implies changes in the magnetization as well as the density. But we may assume that these distortions are still of order $\frac{a_c^2}{r^2}n_0$. The majority of the "pulp" in a molecule's core consists of points whose distance is of order L_q from the actual vortex cores (the "seeds"), so the amount of distortion can be found by substituting $r = L_q$ from Eq. (18). Using the relation between a_c and β shows that the fractional distortion in the "pulp" regions is of order $\frac{a_c^2}{r^2}n_0 \sim (\frac{q}{n_0\beta})^2$, to be com-

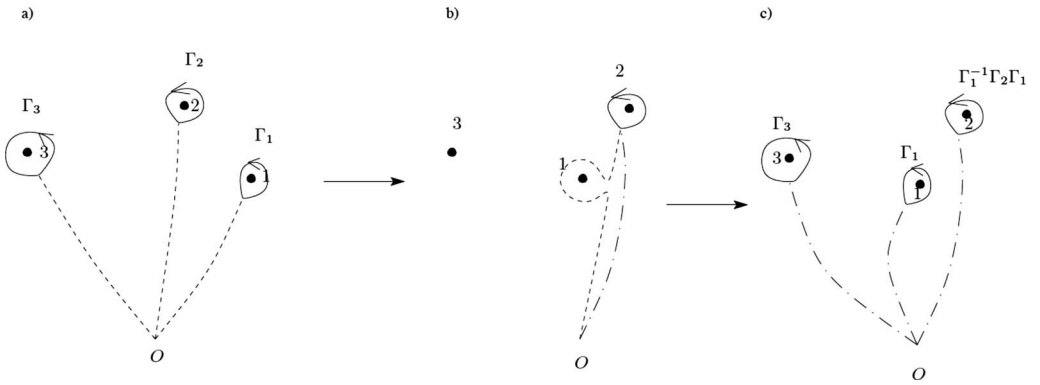

FIG. 10. Changes in the charge assigned to a moving vortex. (a) The convention for assigning vortex charges in the initial configuration. Tethers are drawn directly from the origin to an anchor just below each vortex. As long as the tethers are moved continuously, the correspondence between the tetrahedral state at the anchor and the standard tetrahedral state does not change, so the charges do not change. [(b) and (c)] How the charge of vortex 2 changes when vortex 1 moves below it. Dashed lines in (a) and the dashed-dotted-dashed lines in (c) are the tethers before and after vortex 1 moves. (b) focuses on the tether of vortex 2, showing how the original tether gets pushed to the side by vortex 1 and is replaced by a new tether. Continuing the labeling of the tetrahedron vertices around the original path changes the labeling of the tetrahedron just below vortex 2. Hence the charge of vortex 2 is identified differently in (c).

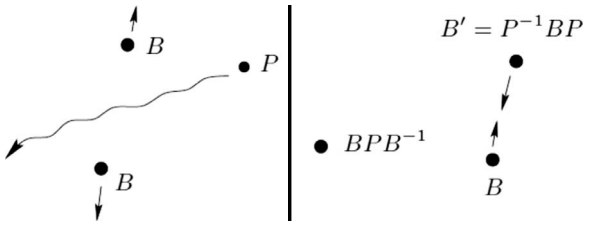

FIG. 11. Catalysis by conjugation; the vortex on the right moves between the other two vortices changing their repulsion to attraction.

pared to the deformations of order $\frac{q}{\beta n_0}$ that result from minimizing Eq. (A5).

APPENDIX B: NONCOMMUTATIVITY OF VORTEX CHARGES

To give a complete description of charge conservation when the charges are described by the noncommuting rotations of a tetrahedron, one needs to give a rule for how to multiply the charges of a set of vortices together to get the net charge. A convention, which we have been using implicitly, is that the topological charges should be multiplied together in the same order that the vortices are arranged along the x axis.

It seems that this definition has an awkward consequence: does the net vortex charge jump suddenly when two of the vortices are reordered because of the noncommutativity of the group of charges? In Fig. 10 vortices 1 and 2 are interchanged between frames (a) and (c), which suggests that the net charge changes from $\Gamma_3\Gamma_2\Gamma_1$ to $\Gamma_3\Gamma_1\Gamma_2$. But this deduction is incorrect and the net vortex charge *is* actually conserved.

The resolution of the paradox has to do with the fact that the charge of a vortex can only be determined up to conjugacy, unless one introduces a systematic convention. For example, the charge of a 120°-rotation vortex is ambiguous—the rotation could be either P, Q, R, or S, and there is no way to distinguish between these because the four vertices of the tetrahedra are indistinguishable. (Abstractly speaking, the four rotations are conjugate elements of the group.) In order to identify the charge of each vortex, we have to choose a routine for labeling the vertices of the tetrahedra nearby. Here is the convention that is consistent with the rule above for ordering the vortex charges. Take a point O far below all the vortices in the system and connect it with lines to points just below the vortices [see Fig. 10(a)]. Now identify the *base* tetrahedron at O with the standard tetrahedron in Fig. 2(a), making a choice from among the 12 possible ways. The labeling at O can be communicated to the tetrahedron at the end point of each line, by copying the labeling from O to a nearby tetrahedron on the line, and then continuing to copy the labeling until the end of the line is reached. Now the charge of a vortice can be identified by using the labeling of the nearby tetrahedron to assign a letter to its rotation axis.

Now that we have a consistent convention for assigning vortex charges, we can show that the net charge of a set of vortices does not change when two of them are interchanged. The trick is that the charges of the *individual* vortices do change in such a way that the product charge does not change. Between Figs. 10(a) and 10(c), vortex 2 is moved over vortex 1. Because vortex 2's tether gets tangled up with vortex 1 when vortex 1 passes below it, its charge gets redefined, as $\Gamma_1^{-1}\Gamma_2\Gamma_1$. The other two vortices' charges do not change. The net charge, obtained by multiplying the vortex charges from left to right, is

$$\Gamma_3\Gamma_1(\Gamma_1^{-1}\Gamma_2\Gamma_1) = \Gamma_3\Gamma_2\Gamma_1. \tag{B1}$$

Thus the net charge does not change. On the other hand, there is a sudden jump in the charge of vortex 2, but this does not mean that the fields of tetrahedra are changing suddenly; the vortex has just been reclassified, with a vortex charge that is conjugate to the original charge.

Here is an interesting consequence of the noncommuting charges: the force between a pair of vortices changes from repulsive to attractive if a third vortex wanders between them. In Fig. 11 one vortex (the P one) catalyzes a reaction without touching the other two vortices involved. (Assume the phases are 0 for the two B vortices and $\frac{2\pi}{3}$ for the P vortex.) To figure out what happens, keep track of when a vortex's connection to the reference point (below the figure) is interrupted by another vortex. The charge of the vortex passing underneath is not changed and the charge of the vortex on top changes to keep the total charge the same. This information is sufficient for working out all the charges. When P passes below the B on the right, the latter vortex changes to a $B'=P^{-1}BP$, so that the net charge is still the same even though P has moved. (This can be used to work out the charges: the net charge of the two vortices which have switched has to be the same so $PB'=BP$ and $B'=P^{-1}BP$.) Next, P passes *above* the B on the left, and the *former* vortex changes to a BPB^{-1} vortex. Now the SU_2 matrices for B and P are $-i\sigma_y$ and $\frac{1-i\sigma_x+i\sigma_y+i\sigma_z}{2}$ (using the axes associated with χ_2). Multiplying out the charges shows that $B'=A^{-1}$. The force between the original pair of vortices (say the P is far away at the beginning and end) is $\frac{n_0\hbar^2\pi}{mL}[I_E(B^2,0)-I_E(B,0)-I_E(B,0)]$ and the force between the vortices they turn into is $\frac{n_0\hbar^2\pi}{mL}[I_E(BA^{-1},0)-I_E(A^{-1},0)-I_E(B,0)]$. ($L$ is the distance between the vortices.) The vortices repel each other at first, but after P's intervention, they attract each other, as one sees by checking that $BA^{-1}=C$ and that B^2 is a 2π rotation with energy index 2 while the other reacting charges are all π rotations, with index $\frac{1}{2}$.

We have been assuming that $q=0$, but a similar reaction could also happen in the core of a composite vortex when $q\neq 0$; that is why one has to check all the possible ways for vortices to wander around one another before coalescing or before dividing into groups.

[1] S. Chandrasekhar, *Liquid Crystals* (Cambridge University Press, Cambridge, 1994).
[2] I. Chuang, R. Durrer, N. Turok, and B. Yurke, Science **251**, 1336 (1991).
[3] C. J. Pethick and H. Smith, *Bose-Einstein Condensation in Dilute Gases* (Cambridge University Press, Cambridge, England, 2002).
[4] L. P. Pitaevskii and S. Stringari, *Bose-Einstein Condensation* (Clarendon, Oxford, 2003).
[5] J. Stenger, S. Inouye, D. Stamper-Kurn, H.-J. Miesner, A. Chikkatur, and W. Ketterle, Nature (London) **396**, 345 (1998).
[6] T.-L. Ho, Phys. Rev. Lett. **81**, 742 (1998).
[7] T. Ohmi and K. Machida, J. Phys. Soc. Jpn. **67**, 1822 (1998).
[8] L. E. Sadler, J. M. Higbie, S. R. Leslie, M. Vengalattore, and D. M. Stamper-Kurn, Nature (London) **443**, 312 (2006).
[9] M. Lewenstein, A. Sanpera, V. Ahufinger, B. Damski, A. S. De, and U. Sen, Adv. Phys. **56**, 243 (2007).
[10] I. Bloch, J. Phys. B **38**, S629 (2005).
[11] C. V. Ciobanu, S.-K. Yip, and T.-L. Ho, Phys. Rev. A **61**, 033607 (2000).
[12] N. D. Mermin, Rev. Mod. Phys. **51**, 591 (1979).
[13] M. M. Salomaa and G. E. Volovik, Rev. Mod. Phys. **59**, 533 (1987).
[14] Grigory E. Volovik, *The Universe in a Helium Droplet* (Clarendon, Oxford, 2003).
[15] P. J. Hakonen, M. Krusius, M. M. Salomaa, J. T. Simola, Yu. M. Bunkov, V. P. Mineev, and G. E. Volovik, Phys. Rev. Lett. **51**, 1362 (1983).
[16] J. S. Korhonen, Y. Kondo, M. Krusius, E. V. Thuneberg, and G. E. Volovik, Phys. Rev. B **47**, 8868 (1993).
[17] K. Kasamatsu, M. Tsubota, and M. Ueda, Phys. Rev. Lett. **93**, 250406 (2004).
[18] T. Isoshima and S. Yip, J. Phys. Soc. Jpn. **75**, 074605 (2006).
[19] Y. Zhang, H. Mäkelä, and K. Suominen, Chin. Phys. Lett. **22**, 536 (2005); see also arXiv:cond-mat/0305489.
[20] G. W. Semenoff and F. Zhou, Phys. Rev. Lett. **98**, 100401 (2007).
[21] H. Makela and K. A. Suominen, Phys. Rev. Lett. **99**, 190408 (2007).
[22] C. Wu, Mod. Phys. Lett. B **20**, 1707 (2006).
[23] D. Controzzi and A. M. Tsvelik, Phys. Rev. Lett. **96**, 097205 (2006).
[24] V. Pietila, M. Mottonen, T. Isoshima, J. A. M. Huhtamaki, and S. M. M. Virtanen, Phys. Rev. A **74**, 023603 (2006).
[25] M. Uhlmann, R. Schützhold, and U. R. Fischer, Phys. Rev. Lett. **99**, 120407 (2007).
[26] A. Lamacraft, Phys. Rev. Lett. **98**, 160404 (2007).
[27] R. W. Cherng, V. Gritsev, D. M. Stamper-Kurn, and E. Demler, Phys. Rev. Lett. **100**, 180404 (2008).
[28] A. Lamacraft, Phys. Rev. A **77**, 063622 (2008).
[29] M. Moreno-Cardoner, J. Mur-Petit, M. Guilleumas, A. Polls, A. Sanpera, and M. Lewenstein, Phys. Rev. Lett. **99**, 020404 (2007).
[30] M. Vengalattore, S. R. Leslie, J. Guzman, and D. M. Stamper-Kurn, Phys. Rev. Lett. **100**, 170403 (2008).
[31] K. Gross, C. P. Search, H. Pu, W. Zhang, and P. Meystre, Phys. Rev. A **66**, 033603 (2002).
[32] K. Kasamatsu, M. Tsubota, and M. Ueda, Int. J. Mod. Phys. B **19**, 1835 (2005).
[33] R. Barnett, S. Mukerjee, and J. E. Moore, Phys. Rev. Lett. **100**, 240405 (2008).
[34] A. E. Leanhardt, A. Gorlitz, A. P. Chikkatur, D. Kielpinski, Y. Shin, D. E. Pritchard, and W. Ketterle, Phys. Rev. Lett. **89**, 190403 (2002).
[35] A. E. Leanhardt, Y. Shin, D. Kielpinski, D. E. Pritchard, and W. Ketterle, Phys. Rev. Lett. **90**, 140403 (2003).
[36] Y. Shin, M. Saba, M. Vengalattore, T. A. Pasquini, C. Sanner, A. E. Leanhardt, M. Prentiss, D. E. Pritchard, and W. Ketterle, Phys. Rev. Lett. **93**, 160406 (2004).
[37] U. A. Khawaja and H. T. C. Stoof, Phys. Rev. A **64**, 043612 (2001).
[38] H. Zhai, W. Q. Chen, Z. Xu, and L. Chang, Phys. Rev. A **68**, 043602 (2003).
[39] H. T. C. Stoof, E. Vliegen, and U. Al Khawaja, Phys. Rev. Lett. **87**, 120407 (2001).
[40] Y. Kawaguchi, M. Nitta, and M. Ueda, Phys. Rev. Lett. **100**, 180403 (2008).
[41] R. Barnett, A. Turner, and E. Demler, Phys. Rev. Lett. **97**, 180412 (2006).
[42] R. Barnett, A. Turner, and E. Demler, Phys. Rev. A **76**, 013605 (2007).
[43] J. Kronjager, C. Becker, P. Navez, K. Bongs, and K. Sengstock, Phys. Rev. Lett. **97**, 110404 (2006).
[44] M.-S. Chang, C. D. Hamley, M. D. Barrett, J. A. Sauer, K. M. Fortier, W. Zhang, L. You, and M. S. Chapman, Phys. Rev. Lett. **92**, 140403 (2004).
[45] A. Widera, F. Gerbier, S. Fölling, T. Gericke, O. Mandel, and I. Bloch, New J. Phys. **8**, 152 (2006).
[46] H. Schmaljohann, M. Erhard, J. Kronjäger, M. Kottke, S. van Staa, L. Cacciapuoti, J. J. Arlt, K. Bongs, and K. Sengstock, Phys. Rev. Lett. **92**, 040402 (2004).
[47] D. M. Stamper-Kurn and W. Ketterle, in *Coherent Atomic Matter Waves-Ondes de Matiere Coherentes*, edited by R. Kaiser, C. Westbrook, and F. David, Proceedings of the Les Houches Summer School of Theoretical Physics, LXXII (Springer-Verlag, Berlin, 1999).
[48] The α's for this vortex may be calculated by noting that, relative to the tetrahedron, the z axis of space rotates 180° about A so that $(\cos\alpha_1, \cos\alpha_2, \cos\alpha_3)$ its coordinates relative to the body axes of the tetrahedron are easy to work out as functions of ϕ.
[49] D. R. Nelson, *Defects and Geometry in Condensed Matter Physics* (Cambridge University Press, Cambridge, England, 2002).
[50] Ryan Barnett (private communication).
[51] Spin vortices in ferromagnetic condensates (Refs. 6 and 7) can be identified because the magnetization drops to zero inside of them.
[52] M. Ueda and M. Koashi, Phys. Rev. A **65**, 063602 (2002).
[53] For zero net magnetization, domains will have to form to conserve the spin. Even when the cubic Zeeman term is taken into account, one can show that there is a discontinuous phase transition (as the thermodynamical variable conjugate to magnetization is varied) although the symmetry between $\pm\hat{z}$ is not exact.
[54] D. R. Tilley and J. Tilley, *Superfluidity and Superconductivity*, 3rd ed. (Institute of Physics Publishing, Bristol, 1990).
[55] In fact, if h is any function that is increasing and convex then the curve $F_{\min}(\phi)$ minimizing $A(F)=\int_0^{2\pi} d\phi h(|F'(\phi)|)$ for fixed end points is a geodesic. This minimization problem can be broken into two steps. First, for a given trajectory, find the best way to trace it out. If F describes uniform motion along the curve, then $A(F)$ is smaller than any kind of intermittent motion. For uni-

form motion, the value of $A(F)$ is clearly $2\pi h(\frac{l}{2\pi})$, where l is the length of the curve. Second, find the trajectory that minimizes A for uniform motion; this is tantamount to minimizing l so the trajectory is a geodesic.

[56] S. Chandrasekhar and G. S. Ranganath, Adv. Phys. **35**, 507 (1986).

[57] For more than two vortices, the remainder f makes a significant contribution to the *force* on a vortex because the logarithmically divergent terms which dominate it in the *energy* are just additive constants. If f is complicated enough, the combination of the Zeeman and kinetic energies might have several local minima, corresponding to different "stereoisomers" for a vortex molecule for a vortex molecule.

[58] Discussions with Joel Moore and Subroto Mukerjee.

[59] Some calculations the authors have worked on suggest that the breakup only lowers the net energy by a *finite* amount, about $\pi\frac{n_0\hbar^2}{m}\ln\sqrt{\frac{\alpha}{\beta}}$, and that the fragments interact with a short-range repulsion, $\propto \ln r/r^3$; in contrast, when the energy index of the fragments actually decreases the force is $\propto \frac{1}{r}$.

[60] Paolo Biscari and Giovanna Guidone Peroli, Commun. Math. Phys. **186**, 381 (1997).

[61] M. F. Andersen, C. Ryu, P. Clade, V. Natarajan, A. Vaziri, K. Helmerson, and W. D. Phillips, Phys. Rev. Lett. **97**, 170406 (2006).

[62] T. Isoshima, K. Machida, and T. Ohmi, J. Phys. Soc. Jpn. **70**, 1604 (2001).

[63] Hence, the direction of the magnetization, $\hat{\boldsymbol{n}}$, helps determine the orientation of the tetrahedra near each vortex core in spite of the pseudoisotropy described by Eq. (51). If there are several vortices nearby one can try to guess how the tetrahedron fields around them fit together.

[64] S. Stock, Z. Hadzibabic, B. Battelier, M. Cheneau, and J. Dalibard, Phys. Rev. Lett. **95**, 190403 (2005).

[65] A. Griesmaier, J. Werner, S. Hensler, J. Stuhler, and T. Pfau, Phys. Rev. Lett. **94**, 160401 (2005).